DETERMINATION OF DEGREE OF ANISOTROPY OF KTP CRYSTAL USING REFLECTANCE ANISOTROPY SPECTROSCOPY TECHNIQUE

By
Fekadu Gashaw

A THESIS PRESENTED TO
THE SCHOOL OF GRADUATE STUDIES
ADDIS ABABA UNIVERSITY
IN PARTIAL FULFILLMENT OF THE REQUIREMENTS
FOR THE DEGREE OF

MASTER OF SCIENCE in PHYSICS

ADDIS ABABA, ETHIOPIA
JUNE 2006

ADDIS ABABA UNIVERSITY

DEAPRMENT OF PHYSICS

The undersigned hereby certify that they have read and recommend to the Faculty of Science for acceptance a senior project entitled "**Determination of Degree of Anisotropy of KTP crystal using Reflectance Anisotropy Spectroscopy Technique** " by **Fekadu Gashaw Master of Science**.

Dated: June 2006

Supervisor: _____

Dr. Araya Asfaw

Readers: _____

Dr. Dereje Ayalew

_____

Dr. Mebratu G/mariam

ADDIS ABABA UNIVERSITY

Date: **June 2006**

Author: **Fekadu Gashaw**

Title: **Determination of Degree of Anisotropy of KTP crystal using Reflectance Anisotropy Spectroscopy Technique**

Department: **Deaprment of Physics**

Degree: **M.Sc.** Convocation: **July** Year: **2006**

_____

Signature of Author

This Work is Dedicated to

My parents and Feru

Table of Contents

List of Tables

List of Figures

Acknowledgements

It is my pleasure to express warm appreciation to my adviser Dr. Araya Asfaw, for his continuous assessment from the scratch until I wind up my work. He also provided me with different supporting materials which are used as a base for this thesis. I am especially grateful to Dr. Mesfine Redi, my co-adviser, for his unreserved advise and suggestions almost in all parts of my experimental work. Here, I can say that his suggestion and constructive criticism made this paper to stand one step a head. My thanks passe to prof. Tony Philpotts, in addition sending me different useful articles, his immediate response, whenever I face problem during my work, make me strong. In addition, I would like to thank Prof. Gholap, who has discussed important points about my problem. Some times words are really too poor to express ones feeling about few special persons like my unforgettable friends Tesfaye Mamo and Abraham Aklog. It is not exaggeration to say that, without their technical and friendly support this thesis would never have seen the light of day. Furthermore, I would like to thank Ato Sintayehu Tesfa, for his willingness to see and giving me valuable suggestions on the manuscript of this paper. Asmamaw Molla and Dill Betegle I value yours help greatly.

Fekadu Gashaw

June, 2006

Abstract

Reflectance anisotropy spectroscopy (RAS) is a non-distractive optical probe of surfaces that is capable of operation within a wide range of environments. In this thesis by applying this optical technique it has been attempted to determine the degree of anisotropy of the biaxial Potassium Titanyl Phosphate (KTP) crystal with fractional error 0.165 %. In addition, the angle between the two optical axes of KTP crystal has been calculated with mean error 0.16 % for the case of acute angle and 0.17% mean error for obtuse angle. Furthermore, attempt was made to apply the method to natural basalt rock which is found from Ertal' Ale eastern part of Ethiopia.

INTRODUCTION

When electromagnetic wave interact with crystal a number of important optical properties will be observed. Crystal is a three-dimensional representation of some unit of atoms or molecules whose microscopic structure is characterized by a periodic representation in three dimensions of a motif composed of atoms. In the case of quartz, for example, the motif is made up of three silicon atoms and six oxygen atoms and occupies a volume of $0.113nm^3$. Thus crystals have ordered structure and the study of order and disorder is a central preoccupation of the crystallographer. The periodic structure of crystals at the atomic level affects their macroscopic and physical properties. Properties that are not directional dependent are termed isotropic; those which are directional are termed anisotropic. According to an ancient definition, crystal is a body which is both homogeneous and anisotropic.

Anisotropic crystalline matter has a number of properties which are dependent on the direction of observation. Thus, electrical conductivity may depend on the orientation of the electrical potential applied to the crystal; Young's modulus which describes the linear strain of a material resulting from a linear stress is equally a function of direction. Anisotropy is also the source of characteristic properties that are lacking in isotropy materials. As example, one may consider piezoelectricity and birefringence. With the longitudinal effects, additional transverse effects may occur. In a crystal, an electric current dose not necessarily flow parallel to the applied electric field. In general, a crystal under a longitudinal stress will under go not only a longitudinal dimension change but shear [1].

In most cases anisotropy materials exhibit nonlinear effects; that is the phase velocity of light waves in nonlinear material varies with the direction of propagation and the polarization of the wave. Thus, the phenomena which will now be described are derived from nonlinear polarization of material media. The effects depend on the crystal structure and are absent in isotropic media and centrosymmetric crystals. The possibility of nonlinear interactions of beams of light to produce second harmonic generation (SHG) and other observable effects will be mentioned later on . In this thesis it has been attempted to determine the

degree of anisotropy of the KTP crystal which has so many optical importance.

Potassium Titanyl Phosphate-KTP crystal

Potassium titanyl phosphate ($KTiOPO_4$;KTP) was first synthesized in 1890 by L.Ouvard. But its great application was not identified until the 1970's [2]. KTP is a nonlinear optical crystal, which possesses excellent nonlinear and electro-optic properties. A combination of high nonlinear coefficient, wide transparency range and broad angular as well as thermal acceptances make KTP very attractive for different nonlinear optical and wave guide applications [3,4]. Its electro-optic wave guide modulator figure of merit that is nearly double that for any other inorganic materials. Further more, it is known as a quasi-one dimensional super-ionic conductor of K^+ ions and it is a room temperature ferroelectric material having a phase transition temperature at $934 \pm 2^0 C$ [5].

Transparency band edges of KTP crystal are at $0.35\mu m$ in UV and $4.4\mu m$ in IR region. Due to very high effective nonlinearity and excellent optical properties of KTP crystal lies in $0.99 - 3.3\mu m$ region. This allows to use KTP as an intarcavity and extracavity frequency doubler for the most commonly used lasers, such as Nd:YAG laser. The vary large temperature band-width of KTP is particularly advantageous for maintaining pulsed energy stability of the converted beam. Due to this feature and good thermal properties, KTP has an exceptional figure of merit for doubling of high average power (cw or quasi-cw lasers). Thus relatively high bulk damage threshold combined with a low absorption loss at $1\mu m$, renders this material a prime choice for all intracavity frequency doubling applications [3].

KTP belongs to the family of isomorphic compounds with the general composition of MTiOX , where X= P or As and M= K, Rb, NH_4 , Tl or Cs (for X= As only) [4]. Solid solutions exist among the various members of this family, with only slight changes in lattice parameters. All members are orthorhombic and belong to the a centric point group mm2 and space group $Pna2_1$ at room temperature. For KTP the lattice constants are a= 12.814 A^0, b= 6.404 A^0 and c= 10.616 A^0, and each unit cell contains eight formula units. Its complicated characterized by chains of TiO_6 octahedral linked at two corners by alternating long and short Ti-O bonds that give rise to the large nonlinear optical effects observed in KTP [2,4,6].

The application of KTP requires crystals of high perfection of sufficient size. Basically, KTP crystals are grown by hydrothermal and flux methods. Here the later one is a promising method, because large size optical quality crystal can be grown at normal atmospheric conditions without incorporating water molecule which give rise to considerable absorption in infrared region [5].

The KTP crystal morphology is similar for both flux and hydrothermal-growth processes and specifies depend on seed size and orientation. The morphology is shown in fig.1.1.

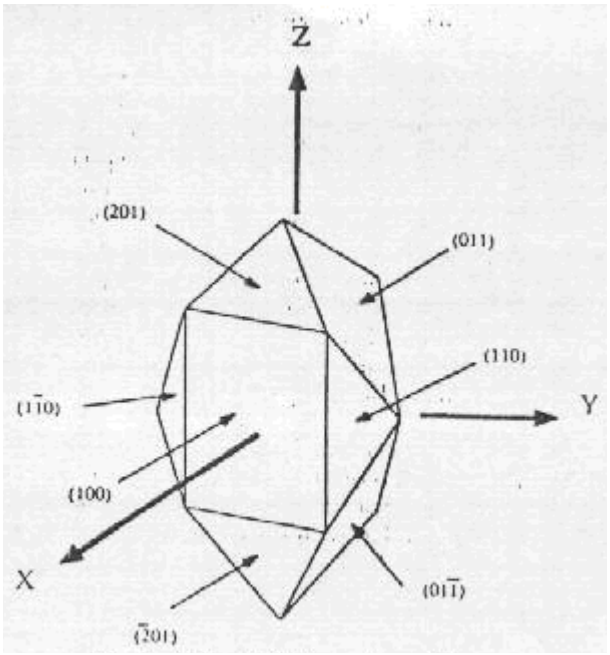

Figure 1: *Natural KTP crystal morphology* .

Here generally it consists of (100), (201) and (011) series of planes that form relatively sharp caps along the c or polar axis and of the (011) and (110) series of planes that form shallower caps along b axis, other higher-order phases can also be present but usually these form smaller faces. the (100) planes form natural

surfaces that readily cleave at room temperature when mild concentrated pressure is applied. Phase matching for various nonlinear processes requires propagation in the principal planes. The natural crystal morphology permits long phase and large apertures to be obtained in this directions when natural (100), (201) and (011) entrance and exit faces are used [6]. All the above mentioned superior properties of KTP crystal is coming from its anisotropy properties, Therefore, all those superior properties of KTP crystal make the writer's to be interested to measure its degree of anisotropy and other related physical quantities.

This thesis is organized in five chapters. The first chapter generally deal with the interaction of matter with light. The optical properties of matter are interpreted on the basis of the electromagnetic theory of light by using Maxwell's equations. Then the nature of electromagnetic wave has been discussed when it propagate through isotropic and anisotropic medium. After that Fresnel coefficients are derived and explained to calculate reflectance of reflected light. In the second chapter the phenomena of polarization is discussed by considering different states of polarization. In addition, the state of polarization was expressed mathematically by applying Jones calculus and Stok's vectors. The basic principles of Reflectance Anisotropy Spectroscopy (RAS) is introduce in the third chapter. In the fourth chapter the experimental results will be discussed and interpreted based on the experimental data. The final chapter of this thesis consists a brief summery and conclusion based on the experimental results.

Chapter 1

LIGHT AND MATTER

1.1 Maxwell's Equation

When one applied Reflectance anisotropy spectroscopy (RAS) as an optical technique it wouldn't give any sense without considering Maxwell's equations. The two concepts with which Maxwell was chiefly concerned and which were well established before his electromagnetic theory were both associated with magnetic fields in the vicinity of conductors. The first of these is Ampere's circuital law, the second is Neumann's equation which followed Faraday's laws of electromagnetic induction [7], and he was also consider Gauss's law as well as continuity equation .

In general the propagation of light through medium can best be understood in terms of electromagnetic waves, on the other hand, the behavior of the electric field $\overrightarrow{E}$ and magnetic field $\overrightarrow{H}$, which are independent of one another can be described by a total of four equations. Two of which relate $\overrightarrow{E}$ and $\overrightarrow{H}$ through a charge density (ρ) and current density $(\overrightarrow{J})$.

For a neutral dielectric medium (one with no free charges) Maxwell's equations are

$$\nabla \overrightarrow{D} = 0, \tag{1.1}$$

$$\nabla \overrightarrow{B} = 0, \tag{1.2}$$

$$\nabla \times \overrightarrow{E} = -\frac{\partial \overrightarrow{B}}{\partial t}, \tag{1.3}$$

$$\nabla \times \overrightarrow{H} = \frac{\partial \overrightarrow{D}}{\partial t} + \overrightarrow{J}. \tag{1.4}$$

Here non magnetic media will be considered for which

$$\overrightarrow{B} = \mu_0 \overrightarrow{H}. \tag{1.5}$$

On the other hand, the electric displacement vector $\overrightarrow{D}$ is defined as

$$\overrightarrow{D} = \epsilon_0 \overrightarrow{E} + \overrightarrow{P}, \tag{1.6}$$

where the polarization $\overrightarrow{P}$ is the electric dipole moment per unit volume of the medium. Polarization is the only term in the Maxwell equations relating directly to the medium. Now, if one substitute Eqs.(1.5) and (1.6) into Eqs.(1.1) to (1.4), the Maxwell's equations can be rewritten as

$$\nabla \overrightarrow{E} = -\frac{1}{\epsilon_0} \nabla \overrightarrow{P}, \tag{1.7}$$

$$\nabla \overrightarrow{H} = 0, \tag{1.8}$$

$$\nabla \times \overrightarrow{E} = -\mu_0 \frac{\partial \overrightarrow{H}}{\partial t}, \tag{1.9}$$

$$\nabla \times \overrightarrow{H} = \epsilon_0 \frac{\partial \overrightarrow{H}}{\partial t} + \frac{\partial \overrightarrow{P}}{\partial t} + \overrightarrow{J}. \tag{1.10}$$

In order to obtain the general wave equation for the electric field the curl of Eq.(1.9) is taken, then substituting Eq.(1.10) to eliminate magnetic field $\overrightarrow{H}$ i.e.

$$\nabla \times (\overrightarrow{\nabla} \times \overrightarrow{E}) + \frac{1}{c^2} \frac{\partial^2 \overrightarrow{E}}{\partial t^2} = -\mu_0 \left(\frac{\partial^2 \overrightarrow{P}}{\partial t^2} + \frac{\partial \overrightarrow{J}}{\partial t} \right). \tag{1.11}$$

It is also possible to get the general wave equation in terms of magnetic field by taking the curl of Eq.(1.10) then substituting Eq.(1.9) to eliminate electric field.

1.2 Propagation of Light through Medium

The presence of matter affects the propagation of light in many ways. The most common and noticeable effects are:

i) The velocity of the propagating light is smaller in material medium than in empty space. The change in the velocity of light at the surface of the separation between the media gives rise to the phenomena of reflection and refraction.

ii) Part of the energy of light is transformed into heat due to partial absorbtion of the light bean.

iii) The light is partially scattered.

The three effects mentioned above depend on frequency. The frequency dependence of the index of refraction leads to dispersion. On the other hand the frequency dependence of absorption is responsible for the color of most objects. Of course, the propagation of light in material substance is inherently a very complex phenomenon. Because the electromagnetic disturbance at any point of the medium results from the combined effects of primary wave coming from the light source and secondary waves due to the forced oscillations of the microscopic dipoles. Yet many optical phenomena can be explained by a simple theory in which the secondary waves do not appear explicitly [8].

1.2.1 Electromagnetic wave in Isotropic Dielectric Material

In this section, we shall consider the propagations of light waves in homogenous (isotropic) dielectric materials. In the case of isotropic, non conduction medium, electrons are highly bound to the atoms comprising the medium and there is no better direction. Here, see also the mechanical representation of charged harmonic oscillator for the case of isotropic medium in fig.1.1.

Let us assume that the electron of charge **-e** in a dielectric at a distance $\overrightarrow{r}$ from the equilibrium position. Here the macroscopic polarization density is defined as

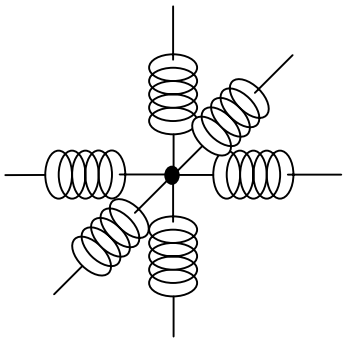

Figure 1.1: *The mechanical oscillator model for an isotropic medium-all the springs are the same, and the oscillator can vibrate equally in all direction.* .

the electric dipole moment per unit volume. If there are N molecules per unit volume, the macroscopic polarization $\overrightarrow{P}$ of the medium is given by

$$\overrightarrow{P} = -Ne\overrightarrow{r}. \tag{1.12}$$

If the displacement of the electron in the above equation comes due to the external static electric field $\overrightarrow{E}$, which is not very much over a distance comparable with the intermolecular distance, and if the electron is elastically bound to its equilibrium position with force constant k, then the force equation would be

$$-e\overrightarrow{E} = k\overrightarrow{r}, \tag{1.13}$$

Form which the position of the electron is found to be

$$\overrightarrow{r} = -\frac{e\overrightarrow{E}}{k}. \tag{1.14}$$

Hence up on substituting Eq.(1.14) in to (1.12), one readily gets

$$\overrightarrow{P} = \frac{Ne^2}{k}\overrightarrow{E}. \tag{1.15}$$

Since the electron is subjected to resistive force, the equation of motion of the

electron is expressed as

$$m\frac{d^2\overrightarrow{r}}{dt^2} + m\gamma\frac{d\overrightarrow{r}}{dt} + k\overrightarrow{r} = -e\overrightarrow{E}, \tag{1.16}$$

where we follow the convention of writing $\overrightarrow{E}$ as $E_0 e^{-i(wt-\overrightarrow{k}z)}$. This means that $\overrightarrow{r}(t)$ in eq.1.16 is also regarded mathematically as a complex quantity in our calculations but only the real part is physically meaningful. This shows both $\overrightarrow{E}$ and $\overrightarrow{r}$ are harmonically time dependent, therefore, eq.1.16 can be rewrite as

$$(-m\omega^2 - im\omega\gamma + k)\overrightarrow{r} = -e\overrightarrow{E}. \tag{1.17}$$

Therefore, $\overrightarrow{r}$ can be given as

$$\overrightarrow{r} = \frac{e\overrightarrow{E}}{m\omega^2 + im\omega\gamma - k}. \tag{1.18}$$

Now Substituting Eq.(1.18) in to (1.12) and results in

$$\overrightarrow{P} = \frac{Ne^2}{-m\omega^2 - im\omega\gamma + k}\overrightarrow{E}. \tag{1.19}$$

The cause of the frictional damping force is the term $m\gamma$ in the denominator in the above equation.The reduced static polarization can be calculated if $\omega = 0$. As it can be easily seen, for a given amplitude of the impressed electric field, the amount of polarization varies with frequency. A more significant way of writing the above equation is:

$$\overrightarrow{P} = \frac{Ne^2}{m(\omega_o^2) - im\omega\gamma}\overrightarrow{E}, \tag{1.20}$$

where ω_0 is the effective resonance frequency of the bound electrons .

$$\omega_0 = \sqrt{\frac{k}{m}}. \tag{1.21}$$

Further more the complex polarizability $\alpha(\omega)$ can be defined as

$$\overrightarrow{P} = \alpha(\omega)\overrightarrow{E}, \tag{1.22}$$

where

$$\alpha(\omega) = \frac{e^2}{m(\omega_0^2 - \omega^2) - i2m\omega\gamma}. \tag{1.23}$$

Here the complex polarization density is given by:

$$\overrightarrow{\mathbf{P}} = N\overrightarrow{P} = N\alpha(\omega)\overrightarrow{E}. \tag{1.24}$$

Using this polarization density in the in homogeneous wave equation i.e

$$\nabla^2\overrightarrow{E} - \frac{1}{c^2}\frac{\partial^2\overrightarrow{E}}{dt^2} = \frac{1}{\epsilon_0 c^2}\frac{d^2\overrightarrow{\mathbf{P}}}{dt^2}, \tag{1.25}$$

it is possible to obtain the following relation by taking $\overrightarrow{E} = E_0 e^{-i(wt-\overrightarrow{k}z)}$, $\nabla^2 \to -k^2$ and $\frac{d^2}{dt^2} \to -\omega^2$

$$(-k^2 + \frac{\omega^2}{c^2})E_0 e^{-i(wt-\overrightarrow{k}z)} = -\frac{\omega^2}{c^2\epsilon_0}.N\alpha(\omega)E_0 e^{-i(wt-\overrightarrow{k}z)}, \tag{1.26}$$

from which the wave number must satisfy the dispersion relation and it can be put in the form i.e

$$k^2 = \frac{\omega^2}{c^2}\left(1 + \frac{N\alpha(\omega)}{\epsilon_0}\right). \tag{1.27}$$

After substitute Eq.(1.23) in to (1.27) one can see that there is an imaginary term in the denominator,which is implies that the wave vector k must be a complex number.

$$k^2 = \frac{\omega^2}{c^2}n^2(\omega), \tag{1.28}$$

which can also be expressed as

$$k = \frac{\omega}{c}n(\omega). \tag{1.29}$$

In this case because $\alpha(\omega)$ is complex, it not difficult to see that, the refractive index is also a complex number.

$$n^2(\omega) = 1 + \frac{Ne^2}{m\omega_0(\omega_0^2 - \omega^2), -i2m\omega_0\gamma\omega} \tag{1.30}$$

$$n^2(\omega) = [n_R(\omega) + in_I(\omega)]^2, \tag{1.31}$$

where n_R and n_I are the real and imaginary parts of the index of refraction respectively.

Here the electric field which is propagating in the medium along z-direction is considered.

$$E(z,t) = E_0 e^{-i(wt-k_z z)}. \tag{1.32}$$

Hence in the view of Eqs.(1.29) and (1.31) one can see that

$$E(z,t) = E_0 e^{-i(wt-\frac{n(\omega)z}{c})} \tag{1.33}$$

which can also be expressed using Eq.(1.31) as

$$\overrightarrow{E}(z,t) = E_0 e^{-n_I(\omega)\frac{\omega z}{c}} \times e^{-i\omega(t-n_R(\omega)\frac{z}{c})} \tag{1.34}$$

Now is is possible to see that E(z,t) is no longer purely oscillatory. Due to $n_I(\omega)$ because the field decay with increasing distance of propagation. Since the intensity is proportional to the square of the electric field, the intensity shows exponential decay with z-direction.

$$I_\omega(z) \propto \overrightarrow{E}^2, \tag{1.35}$$

$$I_\omega(z) = I_\omega(0) e^{-2n_I(\omega)\frac{\omega z}{c}}, \tag{1.36}$$

$$I_\omega(z) = I_\omega(0) e^{-a(\omega)z}, \tag{1.37}$$

where $a(\omega)$ is the absorption coefficient or extinction Coefficient which is given by [9].

$$a(\omega) = \frac{2n_I(\omega)\omega}{c}, \tag{1.38}$$

$$a(\omega) = \frac{2Ne^2}{\epsilon_0 mc} . \frac{\omega^2\gamma}{(\omega_0^2-\omega^2)^2 + 4\gamma\omega^2}. \tag{1.39}$$

It is also possible to verify that the absorption coefficient depends on the wave length of the light as

$$a(\lambda) = \frac{4\pi n_I}{\lambda}. \tag{1.40}$$

Therefore, it can be easily realized that absorption is associated with the complex part of the index of refraction of the material.

1.2.2 Light in Anisotropic Dielectric (crystal) Medium

Until now we have confined our attention to the propagation of light in isotropic media, i.e substances whose optical properties are the same in all directions. Liquids as well as amorphous solid substances such as glass and plastic, are usually isotropic because of the random distribution of the molecules. In many crystals, however, the optical as well as the other physical properties are different along different directions [8].

Anisotropy occurs in the propagation of electromagnetic waves through which an electric field produces a polarization which is not, in general , in the same direction as the electric field. A similar effect might be expected when the magnetic permeability is not a simple scalar quantity, but refractive index is usually determined primarily by the dielectric constant. This occurs for light propagating through crystals and for radio waves propagating through an ionized gas containing a static magnetic field.

In the earlier discussion, our charged oscillator model was characterized by isotropic binding. But now, to portray the optical properties of anisotropic crystal,it is necessary to elaborate bound model oscillators. Therefore, one must ascribe to model oscillating charges i.e, anisotropic binding such as represented by mechanical model of fig.1.2.

A further complication is that the refractive index in any one direction may be a function of the state of polarization of the wave so that a ray entering the medium with a random polarization will be split into two components which will be refracted differently. The medium is then said to be doubly refracting or birefringent. The two components may be plane polarized, as for propagation of light in crystals such as calcite, or circularly polarized, as under some circumstances for the propagation of light in the ionosphere [11,12].

Consequently, the displacement of the electron under the action of an external field $\vec{E}$ depends on the direction of the field as well as its magnitude. This is also

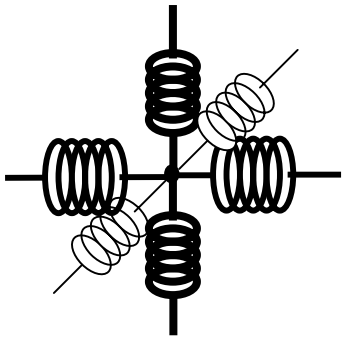

Figure 1.2: *Mechanical model depicting a negatively charged shall bound to positive nucleus for anisotropic medium,where pairs of springs having different stiffness.*

of the resulting polarization $\overline{\mathbf{P}}$. The relation between $\overrightarrow{P}$ and $\overrightarrow{E}$ is expressible as a tensor relation in the form

$$\begin{pmatrix} P_x \\ P_y \\ P_z \end{pmatrix} = \epsilon_0 \begin{pmatrix} \chi_{11} & \chi_{12} & \chi_{13} \\ \chi_{21} & \chi_{22} & \chi_{23} \\ \chi_{31} & \chi_{32} & \chi_{33} \end{pmatrix} \cdot \begin{pmatrix} E_x \\ E_y \\ E_z \end{pmatrix}. \tag{1.41}$$

The above equation can be rewrite as

$$\overrightarrow{P} = \epsilon_0 \chi \overrightarrow{E}, \tag{1.42}$$

where χ is the susceptibility tensor which is given by

$$\chi = \begin{pmatrix} \chi_{11} & \chi_{12} & 13 \\ \chi_{21} & \chi_{22} & \chi_{23} \\ \chi_{31} & \chi_{32} & \chi_{33} \end{pmatrix}. \tag{1.43}$$

In the treatment of isotropic media the displacement $\overrightarrow{D}$ is related to the electric field $\overrightarrow{E}$ by the relation $\overrightarrow{D} = \epsilon \overrightarrow{E}$. Where ϵ is a scaler quantity. $\overrightarrow{D}$ and $\overrightarrow{E}$ being in the same direction. It is found that when an electric field $\overrightarrow{E}$ is established in an optically anisotropic medium, the direction of $\overrightarrow{D}$ does not in general coincide with

that of $\overrightarrow{E}$. The relation between $\overrightarrow{D}$ and $\overrightarrow{E}$ may be exposed by

$$\overrightarrow{D} = \epsilon_0(l + \chi).\overrightarrow{E} = \varepsilon\overrightarrow{E}, \tag{1.44}$$

where, 1 is the unit matrix $\begin{pmatrix} 1 & 0 & 0 \\ 0 & 1 & 0 \\ 0 & 0 & 1 \end{pmatrix}$ and ε= $\epsilon_0(1 + \chi)$, which is the dielectric tensor. For ordinary non-absorbing crystals the χ-tensor is symmetric so that it assumes the diagonal form and the quantities $\mathbf{k}_{11}$ =1+χ_{11}, .., and so forth, are called the principal dielectric constants. In view of Eq.(1.42), the general wave equation in Eq.(1.25) can be written in the form

$$\overrightarrow{\nabla} \times (\overrightarrow{\nabla} \times \overrightarrow{E}) + \frac{1}{c^2}\frac{\partial^2\overrightarrow{E}}{\partial t^2} = -\frac{1}{c^2}\chi\frac{\partial^2\overrightarrow{E}}{\partial t^2}, \tag{1.45}$$

It then follows that the crystal can sustain monochromatic plane waves of the usual form $e^{-i(\overrightarrow{k}.\overrightarrow{r}-wt)}$ provided that the propagation vector $\overrightarrow{k}$ satisfies the condition.

$$\overrightarrow{k} \times (\overrightarrow{k} \times \overrightarrow{E}) + \frac{\omega^2}{c^2}\overrightarrow{E} = -\frac{\omega^2}{c^2}\chi\overrightarrow{E}, \tag{1.46}$$

which is equivalent to

$$\left(-k_y^2 - k_z^2 + \frac{\omega^2}{c^2}\right)E_x + k_xk_yE_y + k_xk_zE_z = -\frac{\omega^2}{c^2}\chi_{11}E_x, \tag{1.47}$$

$$k_yk_xE_x\left(-k_x^2 - k_z^2 + \frac{\omega^2}{c^2}\right)E_y + k_yk_zE_z = -\frac{\omega^2}{c^2}\chi_{22}E_y, \tag{1.48}$$

$$k_zk_xE_x + k_zk_yE_y + \left(-k_x^2 - k_y^2 + \frac{\omega^2}{c^2}\right)E_z = -\frac{\omega^2}{c^2}\chi_{33}E_z, \tag{1.49}$$

In order to interpret the physical meaning of these equations, consider a particular case of a wave propagating in the x-axis. In this case $k_x = k$ and k_y = $k_z = 0$ as a result one can have

$$\tfrac{\omega^2}{c^2}E_x \text{ =- } \tfrac{\omega^2}{c^2}\chi_{11}E_x,$$

$$\left(-k^2+\frac{\omega^2}{c^2}\right)E_y=-\frac{\omega^2}{c^2}\chi_{22}E_y, \tag{1.50}$$

$$\left(-k^2+\tfrac{\omega^2}{c^2}\right)E_z=-\tfrac{\omega^2}{c^2}\chi_{33}E_z,$$

The first equation implies that $E_X=0$, since neither ω nor χ_{11} is zero.This means that the $\overrightarrow{E}$ field is transverse to the x-axis, which is the direction of the propagation. Conceder next the second equation. If $E_y\neq 0$,then

$$K=\frac{\omega}{c}\sqrt{1+\chi_{22}}=\frac{\omega}{c}\sqrt{\mathbf{k}_{22}}, \tag{1.51}$$

The third equation, likewise, implies that if $E_z\neq 0$, then

$$K=\frac{\omega}{c}\sqrt{1+\chi_{33}}=\frac{\omega}{c}\sqrt{\mathbf{k}_{33}}. \tag{1.52}$$

Now $\frac{\omega}{k}$ is the phase velocity of the wave. Thus we have two possible phase velocities, namely,$\frac{c}{\sqrt{\mathbf{k}_{22}}}$ if the $\overrightarrow{E}$ vector points in the y-direction and $\frac{c}{\sqrt{\mathbf{k}_{33}}}$ if the $\overrightarrow{E}$ vector is in the z-direction. More generally it can be shown that for any direction of the propagation vector$\overrightarrow{k}$ there are two possible values of the magnitude k and hence two possible values of the phase velocity. To do this, let us introduce the three principal indices of refraction n_1,n_2 and n_3 defined by

$$n_1=\sqrt{1+\chi_{11}}=\sqrt{\mathbf{k}_{11}},$$

$$n_2=\sqrt{1+\chi_{22}}=\sqrt{\mathbf{k}_{22}}, \tag{1.53}$$

$$n_3=\sqrt{1+\chi_{33}}=\sqrt{\mathbf{k}_{33}}.$$

To get nontrivial solution for E_x,E_y and E_z of Eq.(1.49), the determinant of the coefficients must vanish, i.e

$$\begin{pmatrix} (\frac{n_1\omega}{c})^2-k_y^2-k_z^2 & k_xk_y & k_xk_z \\ k_yk_x & (\frac{n_1\omega}{c})^2-k_x^2-k_z^2 & k_yk_z \\ k_zk_x & k_zk_y & (\frac{n_3\omega}{c})^2-k_x^2-k_y^2 \end{pmatrix}. \tag{1.54}$$

Here, the above equation can be represented by a three-dimensional surface in space. To plot this representation it is necessary to first determine the shape of the wavefront corresponding to a point source in a homogeneous birefringent medium. The wavefront, by definition, is the surface whose points are simultaneously reached by a light wave emitted at a given instant from the velocity of propagation is the same in all directions and the wavefront is spherical, as we know. In an anisotropic medium, however, the wavefront has a more complex shape because the velocity of propagation is different along different directions. Moreover, it is represented by a double surface because, as it has been seen, for each direction there are two possible velocities of propagation, corresponding to two waves with mutually perpendicular planes of vibration (see fig.1.3)

Now conceder any one of the coordinate planes, say the xy plane. In this plane $k_z = 0$, and the determinant in eq.1.54 reduced to the product of the two factors.

$$[(\frac{n_3\omega}{c})^2 - k_x^2 - k_y^2].\{[(\frac{n_1\omega}{c}) - k_y^2].[(\frac{n_2\omega}{c})^2 - k_x^2] - k_x^2 k_y^2\} = 0. \tag{1.55}$$

Since the product must vanish, either or both factors must be zero. Setting the first factor equal to zero gives the equation of circle.

$$k_x^2 + k_y^2 = (\frac{n_3\omega}{c})^2. \tag{1.56}$$

The second factor gives the equation of an ellipse.

$$\frac{k_x^2}{(\frac{n_2\omega}{c})^2} + \frac{k_y^2}{(\frac{n_1\omega}{c})^2} = 1. \tag{1.57}$$

Similarly equations are obtained for the xz and yz planes. The intercept of the $\overrightarrow{k}$ surface with each coordinate plane therefore consists of one circle and ellipse as shown.

The nature of the $\overrightarrow{k}$ surface is such that the inner and outer sheets touch at a certain point P as shown in fig.1.3. This point defines a direction for which the two values of k are equal. That is an optic axis of a crystal, where the phase velocities of the two orthogonally polarized waves reduce to the same value compering to

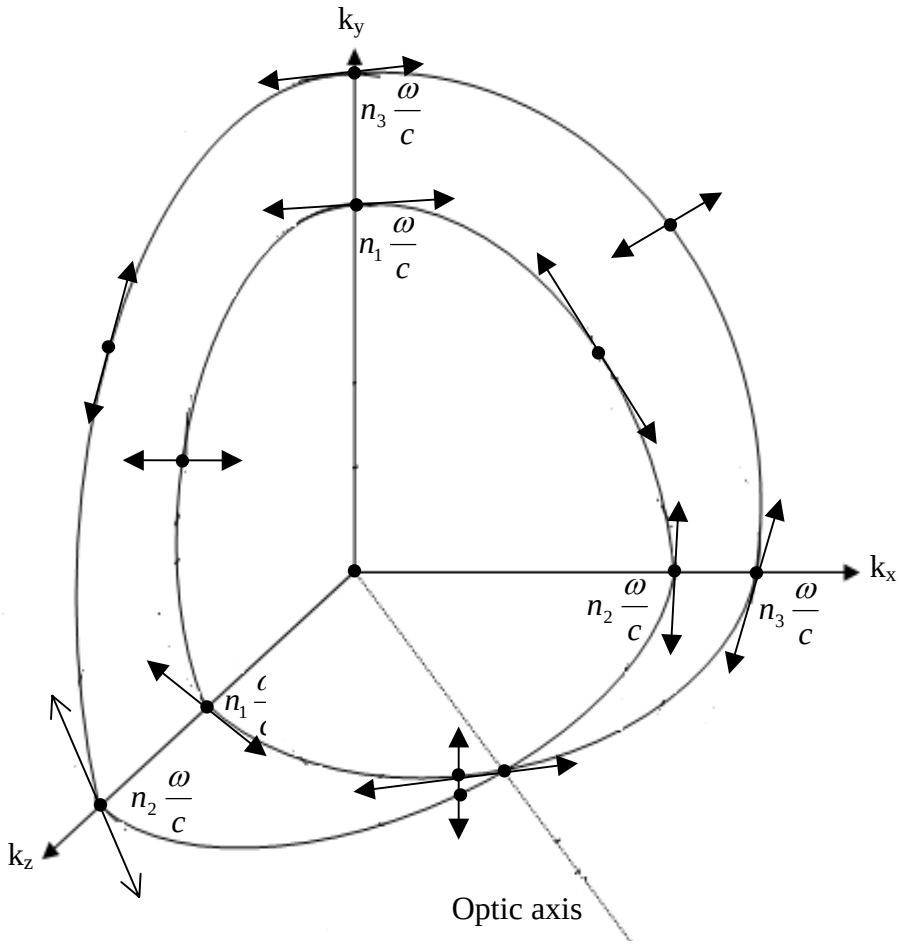

Figure 1.3: *The wave-vector surface.*

other place. Here,we can conveniently classify crystals according to the χ tensor as follows ,see table-1.1:

In a uniaxial crystal the index of refraction that corresponds to the two equal elements, $\chi_{11} = \chi_{22}$ is called ordinary index n_0, which does obey snell's law and the other index, corresponding to χ_{33}, is called the extraordinary index n_E, and does not obey snell's law [1]. If $n_0 < n_E$, the crystal is said to be positive when the velocity of propagation of the extraordinary wave (ν_0) is greatest in the direction of the optic axis and smallest in the directions perpendicular to the optic axis. If $n_0 > n_E$, it is called negative crystal that is the velocity of propagation (ν_0)

Isotropic cubic	$\chi = \begin{pmatrix} a & 0 & 0 \\ 0 & a & 0 \\ 0 & 0 & a \end{pmatrix}$	$\chi_{11} = \chi_{22} = \chi_{33} = a, \quad n = \sqrt{1+a}$
Uniaxial crystal	$\chi = \begin{pmatrix} a & 0 & 0 \\ 0 & a & 0 \\ 0 & 0 & b \end{pmatrix}$	$\chi_{11} = \chi_{22} = a, \quad \chi_{33} = b$ $n_{)} = \sqrt{1+a}$ $n_E = \sqrt{1+b}$
Biaxial crystal	$\chi = \begin{pmatrix} a & 0 & 0 \\ 0 & b & 0 \\ 0 & 0 & c \end{pmatrix}$	$\chi_{11} = a, \ \chi_{22} = b, \ \chi_{33} = c$ $n_1 = \sqrt{1+a}$ $n_2 = \sqrt{1+b}$ $n_3 = \sqrt{1+c}$

Table 1.1: *Classification of crystals according to tensor.*

is minimum in the direction of the optic axis and a maximum in the directions perpendicular to the optic axis see fig.1.4.

To summarize, the wave front developing from a point source in a uniaxial crystal consists of a sphere and of an ellipsoid of revolution around the optic axis. These two surfaces are tangent to each other at the points of intersection with the optic axis. If the crystal is positive, the ellipsoid is prolate and lies inside the sphere (fig.1.4a). If the crystal is negative, the ellipsoid is oblate and encloses the sphere (fgi.1.4b). In biaxial crystal, the shape of the wave front is more complex. If the three characteristic directions are parallel to the x, y and z, axis, respectively, of a Cartesian frame of reference, the intersection of the wave front with each of the three coordinate planes consists of a circle and an ellipse. The wave front does not consist of two separate surface, but of a unique continuous surface folding up on itself and intersecting in a complicated manner [8,10,12,13].

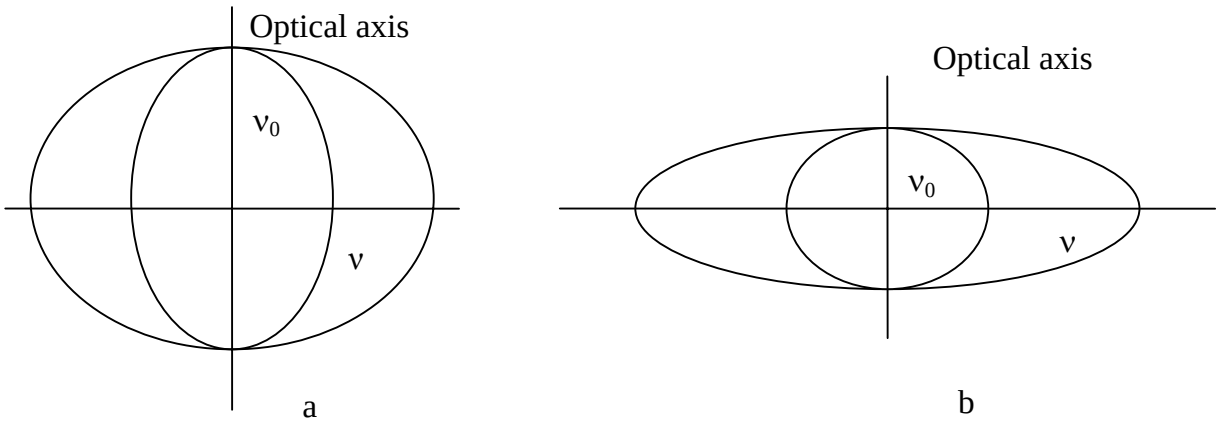

Figure 1.4: *Wave fronts in uniaxial crystal: (a) positive crystal; (b) negative crystal.*

1.3 Reflection and Refraction of light at plane boundary

In this section a basic phenomena of reflection and refraction of light would be investigated from the stand point of electromagnetic theory and applying boundary conditions. Consider a plane harmonic wave incident up on a plane boundary separating two different optical media see fig.1.5. There will be reflected and transmitted wave.

The space-time dependence of these three waves, namely the incident ,reflected and refracted waves , with constant amplitude factors, is given by the following complex expressions respectively:

$$expj(\overrightarrow{k}.\overrightarrow{r} - wt),$$

$$expj(\overrightarrow{k}'.\overrightarrow{r} - wt),$$

$$expj(\overrightarrow{k}''.\overrightarrow{r} - wt).$$

Now, in order that any constant relation can exist for all points of the boundary and for all values of t, it is necessary that the arguments of the three exponential functions be equal at the boundary. Thus since the time factors are already equal,

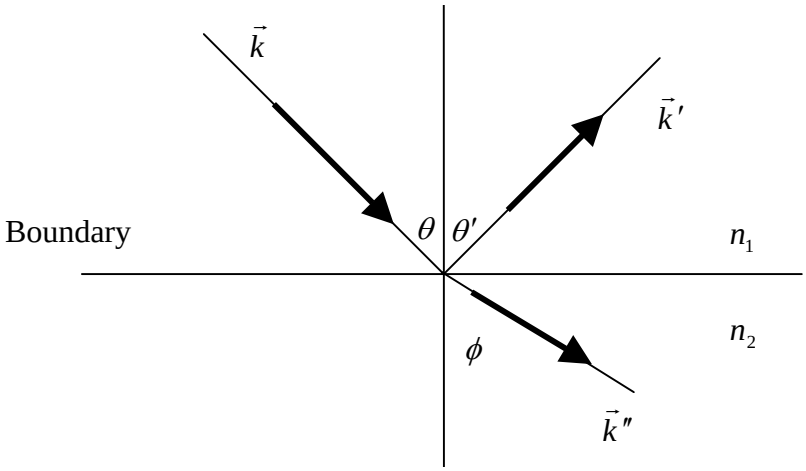

Figure 1.5: *Coordinate system for analyzing reflection and refraction at a plane boundary .*

one may have the following relation at the boundary i.e

$$\overrightarrow{k}.\overrightarrow{r} = \overrightarrow{k}'.\overrightarrow{r} = \overrightarrow{k}''.\overrightarrow{r}. \tag{1.58}$$

These equations imply that all three wave vectors $\overrightarrow{k}, \overrightarrow{k}'$ and $\overrightarrow{k}''$ are coplanar, and their projections on to the boundary plane are all equal. Again choosing a coordinate oxyz such that one of the coordinate planes, say the xz plane, is the boundary, and also the $\overrightarrow{k}$ vector lies in the xy plane, called plane of incidence see again fig.1.5. The angles between the boundary normal (y-axis) and the wave vectors are labelled as θ ,θ' and ϕ as shown. Therefor,Eq.(1.58) becomes

$$ksin\theta = k'sin\theta' = k''sin\phi. \tag{1.59}$$

Now in the space of the incident and reflected waves (y $>$ 0), the two waves are travelling in the same medium but in opposite direction, hence the wave vectors have the same magnitude. i.e , $\overrightarrow{k} = \overrightarrow{k}'$. The first equation then reduces to the familiar law of reflection, which is angle of incidence is the same as angle of

reflection.

$$\theta = \theta'. \tag{1.60}$$

Taking the ratio of the propagation constants of the transmitted wave and the incident wave, we have

$$\frac{\overrightarrow{k}''}{\overrightarrow{k}} = \frac{\frac{\omega}{u''}}{\frac{c}{u}} = \frac{n_2}{n_1} = n, \tag{1.61}$$

where n_1 and n_2 are the indices of refraction of the media, and n is the relative index of refraction. The second part of equation 1.59, therefore, is equivalent to Snell's law of refraction.

$$\frac{Sin\theta}{Sin\phi} = \frac{n_2}{n_1} = n \tag{1.62}$$

Moreover, when the incident beam vibrates in the plane of incidence, there exists a special angle of incidence for which the intensity of the reflected beam drops to zero. In this case the incident beam is totally refracted.

This particular angle of incident is called polarization angle or Brewster's angle. Its value, ϕ_p , is related to the indices of refraction of the two media, n_1 and n_2 , by the following equation:

$$\tan\phi_p = \frac{n_2}{n_1} = n, \tag{1.63}$$

This law is known as Brewster's law.

1.4 Amplitudes of Reflected and Refracted waves

1.4.1 Fresnel Equations

To obtain the amplitudes of reflected and refracted waves, it is mandatory to formulate Fresnel equations to do so,it has been denoted $\overrightarrow{E}$ is the amplitude of electric vector plane harmonic wave that is incident on a plane boundary separating two media, and let$\overrightarrow{E}'$ and $\overrightarrow{E}''$ denote the amplitudes of the reflected and transmitted waves, respectively. Then it follows from the Maxwell curl equations as applied to harmonic waves,Eq.(1.8), that corresponding incident, reflected and

transmitted amplitudes of the magnetic vectors are given follow respectively:

$$\overrightarrow{H} = \frac{\overrightarrow{k} \times \overrightarrow{E}}{\mu, \omega} \tag{1.64}$$

$$\overrightarrow{H}' = \frac{\overrightarrow{k}' \times \overrightarrow{E}'}{\mu, \omega} \tag{1.65}$$

$$\overrightarrow{H}'' = \frac{\overrightarrow{k}'' \times \overrightarrow{E}''}{\mu.\omega} \tag{1.66}$$

It should be noted that the above equations apply either to the instantaneous values of the fields or to the amplitudes, since the exponential factors $expi(\overrightarrow{k}.\overrightarrow{r} - \omega t)$, and so forth are common to both the electric fields and associated magnetic fields.

To find relative magnitudes of the three waves must treat separately the x-components of $\overrightarrow{E}$, which is perpendicular to the plan of incidence (xy-plan) consider fig.1.5. This case is called transverse electric or TE polarization, and that component of $\overrightarrow{E}$,which is parallel to the incidence or the magnetic vector of the incident wave is parallel to the boundary plan. This is called transverse magnetic or TM polarization.For each of these components our boundary conditions require the continuity of the surface (zx-plane) for both the electric and magnetic field vectors.

1) For the normal component of the electric field (TM polarization) it is possible to have the following expiration.

$$\overrightarrow{E} + \overrightarrow{E}' = \overrightarrow{E}''. \tag{1.67}$$

Writing the corresponding equations for the magnetic field vectors, and it can be noticed that they are parallel to the plane of incidence,so that results in

$$-\overrightarrow{H}\cos\theta + \overrightarrow{H}'\cos\theta = -\overrightarrow{H}''\cos\phi,$$

$$-k\overrightarrow{E}\cos\theta + k'\overrightarrow{E}\cos\theta = -k''\overrightarrow{E}''. \tag{1.68}$$

2) For the parallel components of the electric field (TM polarization) the continuity of the horizontal components requires that

$$\overrightarrow{E}\cos\theta + \overrightarrow{E}'\cos\theta = \overrightarrow{E}''\cos\phi, \tag{1.69}$$

and the continuity of the horizontal components of the corresponding magnetic field implies that

$$\overrightarrow{H} - \overrightarrow{H}' = \overrightarrow{H}'',$$

$$K\overrightarrow{E} - K'\overrightarrow{E}' = K''\overrightarrow{E}''. \tag{1.70}$$

Here, it has been used the fact that each magnetic field amplitude $\overrightarrow{H}, \overrightarrow{H}'$ and $\overrightarrow{H}''$ is proportional to $k\overrightarrow{E}, k'\overrightarrow{E}'$ and $k''\overrightarrow{E}''$, respectively as implied by Eqs.(1.64) to (1.66).

The coefficients of reflection $\mathbf{r}_s$ and $\mathbf{r}_p$, and the coefficients of transmission $\mathbf{t}_s$ and $\mathbf{t}_p$ are defined as amplitude ratios, namely

$$\mathbf{r}_s = \left[\frac{\overrightarrow{E}'}{\overrightarrow{E}}\right]_{TE} \qquad \mathbf{r}_p = \left[\frac{\overrightarrow{E}'}{E}\right]_{TM}, \tag{1.71}$$

$$\mathbf{t}_s = \left[\frac{\overrightarrow{E}''}{\overrightarrow{E}}\right]_{TE} \qquad \mathbf{t}_p = \left[\frac{\overrightarrow{E}''}{\overrightarrow{E}}\right]_{TM}. \tag{1.72}$$

Here to eliminate $\overrightarrow{E}''$ from the two sets of Eqs.(1.68) and (1.70) and it is good using the relation $n = \frac{c}{\nu}$ to obtain the following relations for ratios of the reflected amplitudes to the incident amplitudes:

$$\mathbf{r}_s = \frac{\cos\theta - n\cos\phi}{\cos\theta + n\cos\phi}, \tag{1.73}$$

$$\mathbf{r}_p = -\frac{n\cos\theta + \cos\phi}{n\cos\theta + \cos\phi}. \tag{1.74}$$

Ratios for the transmitted amplitudes can be obtained by eliminating $\overrightarrow{E}'$ in the two cases. By using Snell's law in Eq.(1.62), the equations for the amplitudes of the reflected in the form:

$$\mathbf{r}_s = -\frac{\sin(\theta - \phi)}{\sin(\theta + \phi)}, \tag{1.75}$$

$$\mathbf{t}_s = \frac{\cos\theta \sin\phi}{\sin(\theta+\phi)}, \tag{1.76}$$

and

$$\mathbf{r}_p = -\frac{\tan(\theta-\phi)}{\tan(\theta+\phi)}, \tag{1.77}$$

$$\mathbf{t}_p = 2\frac{\cos\theta \sin\phi}{\sin(\theta+\phi)\cos(\theta-\phi)}. \tag{1.78}$$

The above equations are known as Fresnel's equations.They were originally obtained by Fresnel using the elastic-solid theory of light. It should be understood that the elastic-solid theory was never able to give a completely consistent and satisfactory account of reflection and refraction, even when the assumptions concerning the boundary conditions were skilfully adjusted to produce the desired results. The electromagnetic theory does not introduce any special assumptions for this purpose. It uses the standard boundary conditions which are derived from the results of experiments on electricity and magnetism.

For the case of normal incidence $\theta = 0, \phi = 0$, and Fresnel equations give an undetermined results. To investigate this case, it is must convenient to return to the boundary conditions in Eqs.(1.67) and (1.70) which now become:

$$\overrightarrow{E} + \overrightarrow{E}' = \overrightarrow{E}'',$$

and

$$\overrightarrow{E} - \overrightarrow{E}' = \frac{K''}{K} = \frac{n_2}{n_1}.\overrightarrow{E}',$$

from the above equations, one can easily compute the following relations i.e

$$\overrightarrow{E}'' = \frac{2n_1}{n_1+n_2}\overrightarrow{E} \qquad\qquad \overrightarrow{E}' = \frac{n_1-n_2}{n_1+n_2}\overrightarrow{E}. \tag{1.79}$$

The reflectance ρ^2 is the ratio of the intensities of the reflected and incident waves. since the intensity is proportional to the square of the amplitude,its mathematical expiration can be given by

$$\rho^2 = \left|\frac{\overrightarrow{E}'}{\overrightarrow{E}}\right|^2. \tag{1.80}$$

Thus, for example, in the case of perpendicular incidence, we obtain

$$\rho^2 = \left(\frac{n_2 - n_1}{n_2 + n_1}\right)^2 = \left[\frac{n-1}{n+1}\right]^2, \tag{1.81}$$

where, $n = \frac{n_2}{n_1}$, relative index of refraction. The sign of the above equality is negative or positive depending on whether the relative index n is greater or less than unity,respectively. A negative value of $\frac{\vec{E}'}{\vec{E}}$ means that the phase of the reflected wave is changed by 180^0 relative to that of the incident wave. Thus such a change of phase occurs when light is partially reflected upon entering a dense medium [8,10,13,14].

Chapter 2

POLARIZATION OF LIGHT

2.1 Unpolarized Light

One fundamental characteristic of electromagnetic radiation remains to be discussed, that is polarization, and it is rooted in the transverse nature of electromagnetic waves. To see different state of polarization, the nature of unpolarized light is defined initially.

Strictly monochromatic light is fully polarized, though ,it may range anywhere from linear through elliptical to circular polarization. Natural light, on the other hand, is generally found to be unpolarized, for the phase relation between x and y components is totally uncorrelated and phase difference varies rapidly because of this the mean value of phase difference become zero.

Even from the wave-optical point of view natural light is generated in the form of pulses. When caused by narrow spectral lines, these pulses may be of the order of 10^{-8} sec. and contain, say, a million cycles; but even this relatively long period is short compered with the time of observation in the usual optical experiment so that the radiation field observed consists of a large number of pulses whose phases are randomly related. If their angle of polarization:

$$\alpha = \tan^{-1}(\frac{\overrightarrow{E}_y}{\overrightarrow{E}_x}) \qquad -\frac{\pi}{2} < \alpha \leq \frac{\pi}{2}, \tag{2.1}$$

are uniformly distributed over the semicircle, the light will be totally unpolarized. Where $\overrightarrow{E}_x$ and $\overrightarrow{E}_y$ are the x and y components of transverse electromagnetic waves.

The frequency of this light may be 6×10^{14} Hz and its bandwidth one million of that, so that it is monochromatic for many purposes, yet its spectrum band is wide enough to make it unpolarized. Such narrow band width light is same times called quasi-monochromatic [8,14].

2.1.1 Elliptical, Circular and Linear Polarization

Here, a cartesian system of coordinates with the x-axis in the direction of propagation is considered. The y-axis parallel to the optical vector of one wave, and the z-axis parallel to the optical vector of the other wave. The optical vectors of the two waves are represented by expression of the type

$$\overrightarrow{E}_y = A_y \cos[\omega(t - \tfrac{x}{v}) + \psi_1],$$

$$\overrightarrow{E}_z = A_z \cos[\omega(t - \frac{x}{v}) + \psi_2]. \tag{2.2}$$

The functions $\overrightarrow{E}_y$ and $\overrightarrow{E}_z$ also represent the components of the resultant optical vector $\overrightarrow{E}$ along the y and z axes. At a given point in space, this vector varies with time in both length and direction. Its tip describes a curve, of where Eq. (2.2) are the parametric equations. To determine the shape of this curve, we need only t between the two equations. For this purpose we denote $\psi = \psi_2 - \psi_1$, the phase difference between the two oscillations and redefine the origin of time by putting $\omega t' = \omega(t - \frac{x}{v}) + \psi_1$, so Eq.(2.2) becomes to be

$$\overrightarrow{E}_y = A_y \cos(\omega t'),$$

$$\overrightarrow{E}_z = A_z \cos(\omega t' + \psi),$$

$$\overrightarrow{E}_z = A_z \cos\omega t' \cos\psi - Az \sin\omega t' \sin\psi. \tag{2.3}$$

From these equations, one can obtain

$$\frac{\overrightarrow{E}_z}{A_z} - \frac{\overrightarrow{E}_y}{A_y}\cos\psi = -\sin\omega t' \sin\psi. \tag{2.4}$$

Squaring both sides of Eq.(2.4) then the following result will be found.

$$\left[\frac{\overrightarrow{E}_z}{A_z} - \frac{\overrightarrow{E}_y}{A_y}\cos\psi\right]^2 = \sin^2\omega t' \sin^2\psi = \left[1 - \left(\frac{\overrightarrow{E}_y}{A_y}\right)^2\right]\sin^2\psi, \tag{2.5}$$

and, after few reductions it is possible to get the coming expression

$$\frac{E_y^2}{A_y^2} + \frac{E_z^2}{A_z^2} - 2\frac{E_y}{A_y}\frac{E_z}{A_z}\cos\psi = \sin^2\psi. \tag{2.6}$$

This is the equation of an ellipse, and one can conclude that the tip of the vector representing the resultant optical distance at a given point in space describes an ellipse in the plane perpendicular to the direction of propagation. Therefor, this facts expressed by saying that,the wave is Elliptically polarized.

Note that at any instant of time, the magnitude $\overrightarrow{E}$ of the resultant optical disturbance is given by the equation:

$$\overrightarrow{E}^2 = \overrightarrow{E}_y^2 + \overrightarrow{E}_z^2. \tag{2.7}$$

It follows that the intensity (I) of the elliptically polarized wave equals the sum of the intensities (I_y) and (I_z) of the two linearly polarized waves vibrating in the perpendicular planes xy and xz:

$$I = I_y + I_z. \tag{2.8}$$

Thus Eq.(2.2) shows that $\overrightarrow{E}_y$ varies form $+A_y$ to $-A_y$, and $\overrightarrow{E}_z$ varies from $+A_z$ to $-A_z$. Hence, the ellipse represented by these equations, or by Eq.2.6 is inscribed in a rectangle with sides of length $2A_y$ and $2A_z$ see Fig.2.1.

If the two oscillations are in phase, i.e., if ψ equals zero or an even multiple of π, the ellipse degenerates into straight segment, coincident with the diagonal of the rectangle that lays in the first and third quadrants Fig.2.1(b). Indeed, in this

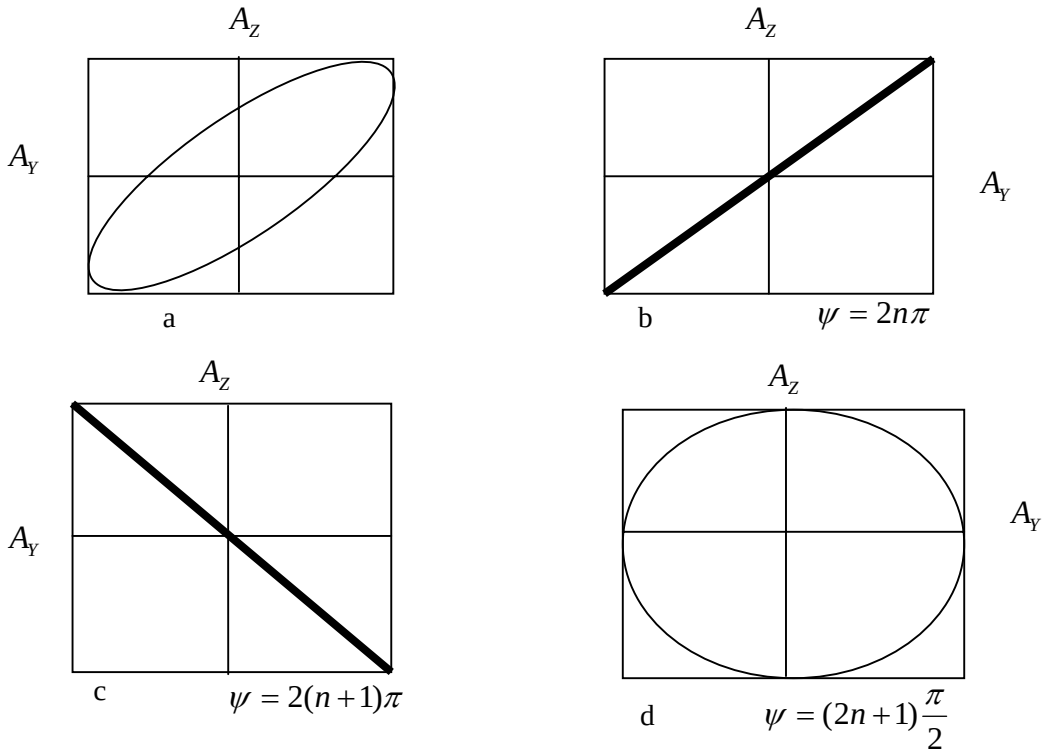

Figure 2.1: States of polarization corresponding to different values of the phase difference ψ .

case Eq.(2.4) yield

$$\frac{E_y}{A_y} = \frac{E_z}{A_z} \qquad \Rightarrow \qquad E_y = \frac{A_y}{A_z} E_z, \tag{2.9}$$

If ψ an odd multiple of π, Eq.2.3 give

$$\frac{E_y}{A_y} = -\frac{E_z}{A_z} \qquad \Rightarrow \qquad E_y = -\frac{A_y}{A_z} E_z. \tag{2.10}$$

The resultant wave is again Linearly polarized, but now the optical disturbance is parallel to the other diagonal of the rectangle i.e, to that lying in the second and fourth quadrants fig.2.1(c). If ψ is an odd multiple of $\frac{\pi}{2}$, Eq.(2.6) becomes

$$\frac{E_y^2}{A_y^2} + \frac{E_z^2}{A_z^2} = 1. \tag{2.11}$$

Which is the equation of an ellipse having its axes in the y and z directions fig.2.1(d). If in particular $A_y = A_z$, the ellipse reduces to a circle and the wave is said to be Circularly polarized. In this condition, the vector representing the optical disturbance at a given point in space rotates with uniform angular speed without change of magnitude.

In the case of elliptical or circular polarization one may in quire in to the direction of rotation of the optical vector. For this purpose consider the positions of the optical vector at time t'=0 and at $t' = \tau$, where τ is a very small fraction of the period T. These positions are shown by the segments op_1, and op_2 in fig.2.2.

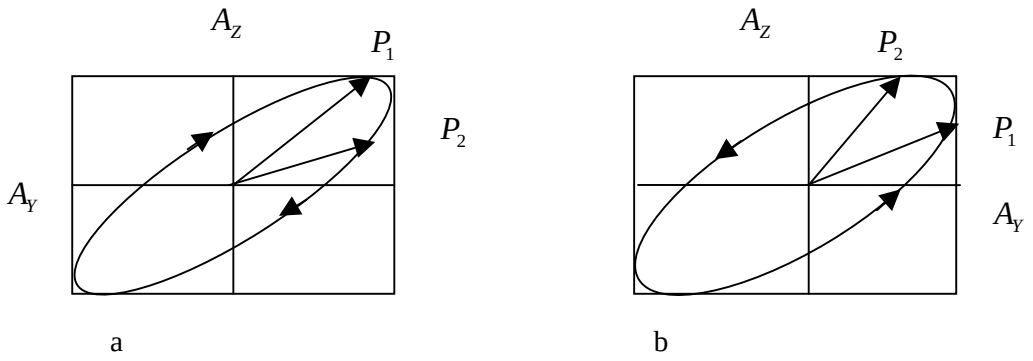

Figure 2.2: (a) $0 < \psi < \pi$; the optical vector rotates clockwise (right-handed polarization). (b) $\pi < \psi < 2\pi$; the optical vector rotates counterclockwise (left-handed polarization).

From Eq.2.3, and considering the above conditions one can obtained the following expressions.

$$at \qquad t' = 0 : \qquad E_y = A_y, \qquad E_z = A_z \cos\psi,$$

$$at \qquad t' = \tau : \qquad E_y = A_y \cos\omega\tau \qquad E_z = A_z \cos(\psi + \omega\tau). \qquad (2.12)$$

It is obvious that, the cosine is a decreasing function of its argument if the argument lies between 0 and π, and an increasing function of its argument if argument lies between 0 and $-\pi$. Thus, if ψ is in the range $0 < \psi < \pi$, $\overrightarrow{E}_z$ is a decreasing function of time $t' = 0$, the point p_2 lies below the point p_1 fig.2.2 (a), and the optical vector rotates clockwise with respect to an observer to ward whom the wave travels. However,if ψ is in the range $-\pi < \psi < 0$, E_z is an optical vector function of time at t' and the optical vector rotates counterclockwise fig.2.2 (b).

In conclusion, for a wave travelling in the direction of the x-axis of a right-handed cartesian frame of reference, the optical vector rotates clockwise or counter clockwise depending whether the z-component leads or lags the y-component by a phase angle less than π. When the rotation is clockwise one can speak of right-handed polarization.When the rotation is counter-clockwise, left-handed polarization will be realized. A phase difference $\psi \pm 2n\pi$, where n is an integer; thus, in particular, one may have left-handed polarization if the z-component leads the y-component by a phase angle between π and 2π [8,12].

2.2 Matrix Representation of Polarization

2.2.1 The Jones Calculus

It is sometimes convenient employ a complex vector amplitude $\overrightarrow{E}_0$ defined as follows

$$\overrightarrow{E}_0 = \overrightarrow{E}_0\mathbf{i} + i\overrightarrow{E}'_0\mathbf{j}, \tag{2.13}$$

the corresponding wave function is

$$\overrightarrow{E} = \overrightarrow{E}_0 expi(\overrightarrow{k}\, z - \omega t). \tag{2.14}$$

This expression can represent any type of polarization. Thus if $\overrightarrow{E}_0$ is real, linear polarization will be found, where as if it is complex, one can see elliptical polarization. In the special case of circular polarization the real and imaginary parts of $\overrightarrow{E}_0$ are equal.

The complex vector amplitude given in Eq.(2.13), is not the most general expression, because it was assumed that the x-component was real and the y-component was imaginary. A more general way of a plane harmonic wave is given by

$$\overrightarrow{E}_0 = E_{0x}\mathbf{i} + iE_{0y}\mathbf{j}, \tag{2.15}$$

where E_{0x} and E_{0y} can both be complex. Accordingly, they can be written in the exponential form as:

$$E_{0x} = |E_{0x}|e^{i\phi_x}, \tag{2.16}$$

$$E_{0y} = |E_{0y}|e^{i\phi_y}. \tag{2.17}$$

A convenient notation for the above pair of complex amplitudes is the following matrix known as Jones vector:

$$\begin{pmatrix} E_{0x} \\ E_{0y} \end{pmatrix} = \begin{pmatrix} |E_{0x}|e^{i\phi_x} \\ |E_{0y}|e^{i\phi_y} \end{pmatrix}, \tag{2.18}$$

where ϕ_x and ϕ_y are the appropriate phases.

If the phaser components E_{0x} and E_{0y} of the Jones vector to assume all possible values at two independent complex numbers, all possible states of polarization of all values of intensity and phase are generated. Here, it is possible to see from table.2.1 how the Jones vector represent the state of polarization.

Where A is the amplitude of the wave at that particular state of polarization. One of the application of the Jones notation is calculating the result of adding two or more waves of given polarizations. The results is obtained simply by adding the Jones vectors. For instant one can easily find the sum of right and left circular polarized waves of equal amplitude. The calculation by means of Jones vectors proceeds as follows:

$$\begin{pmatrix} 1 \\ -i \end{pmatrix} + \begin{pmatrix} 1 \\ i \end{pmatrix} = 2\begin{pmatrix} 1 \\ 0 \end{pmatrix}.$$

The last expression shows that the resultant wave is linearly polarized in x-direction and its amplitude is twice that of either of the circular components.

State of polarization	Jones vector
Linearly polarized in the x-direction.	$\mathrm{A}\begin{pmatrix}1\\0\end{pmatrix}$
Linearly polarized in the y-direction.	$\mathrm{A}\begin{pmatrix}0\\1\end{pmatrix}$
Linearly polarized at 45^0 relative to x-axis	$\mathrm{A}\begin{pmatrix}1\\1\end{pmatrix}$
Left circular polarization	$\mathrm{A}\begin{pmatrix}1\\i\end{pmatrix}$
Right circular polarization	$\mathrm{A}\begin{pmatrix}1\\-i\end{pmatrix}$

Table 2.1: Jones vectors for different states of polarization.

Another use of the matrix notation is computing the effect of inserting a linear optical element, or a train of such elements, in to a beam of light of given polarization. The optical elements are represented by 2×2 matrices that is Jones matrices. The types of optical devices that can be, so represented include linear polarizers, circular polarizers, phase retarders (quarter-wave plates,...), isotropic phase changers and isotropic absorbers.

The matrices are used as follows. Let the vector of the incident light be $\begin{pmatrix}A\\B\end{pmatrix}$ and the vector of the emerging light to be $\begin{pmatrix}A'\\B'\end{pmatrix}$. Then the incident and the emerging light be related as follow i.e

$$\begin{pmatrix}A'\\B'\end{pmatrix} = \begin{pmatrix}a & b\\c & d\end{pmatrix} . \begin{pmatrix}A\\B\end{pmatrix}, \tag{2.19}$$

where $\begin{pmatrix}a & b\\c & d\end{pmatrix}$ is the Jones matrix of the optical element. If light is sent through

a train of optical elements, then the result is given by matrix multiplication:

$$\begin{pmatrix} A' \\ B' \end{pmatrix} = \begin{pmatrix} a_1 & b_1 \\ c_1 & d_1 \end{pmatrix} . \begin{pmatrix} a_2 & b_2 \\ c_2 & d_2 \end{pmatrix} ..... \begin{pmatrix} a_n & b_n \\ c_n & d_n \end{pmatrix} . \begin{pmatrix} A \\ B \end{pmatrix} . \tag{2.20}$$

Here, it should be noted that the Jones calculus is of use only for computing results with light that is initially polarized in some way, that mean, there is no Jones vector representation for unpolarized light [10,15].

2.2.2 Orthogonal Polarization

Two waves whose states of polarization are represented by the complex vector amplitudes $\overrightarrow{E}_1$ and $\overrightarrow{E}_2$ are said to be orthogonally polarization if they have satisfied the following important conditions

$$\overrightarrow{E}_1 . \overrightarrow{E}_2^* = 0. \tag{2.21}$$

Where the asterisk denotes the complex conjugate.

For linearly polarized light , orthogonality merely means that the fields are polarized at right angles to one another. In the case of circular polarization it is readily seen that right-circular and left-circular polarizations are mutually orthogonal states. Similarly, the ellipse of polarization that correspond to two orthogonal Jones vectors have equal and opposite ellipticities (handedness) and their major axes are mutually orthogonal. But, there is a corresponding orthogonal polarization for any type of polarization.

In terms of Jones vectors it is easy to verify that $\begin{pmatrix} A_1 \\ B_1 \end{pmatrix}$ and $\begin{pmatrix} A_2 \\ B_2 \end{pmatrix}$ are orthogonal if and only if

$$A_1 A_2^* + B_1 B_2^* = 0. \tag{2.22}$$

It is instructive to note that light of arbitrary polarization can always be resolved in to two orthogonal components. Thus resolution in to linear components is written

$$\begin{pmatrix} A \\ B \end{pmatrix} = \text{A} \begin{pmatrix} 1 \\ 0 \end{pmatrix} + \text{B} \begin{pmatrix} 0 \\ 1 \end{pmatrix},$$

and in to circular components is written.

$$\begin{pmatrix} A \\ B \end{pmatrix} = \frac{1}{2}(A + iB). \begin{pmatrix} 1 \\ -i \end{pmatrix} + \frac{1}{2}(A - iB). \begin{pmatrix} 1 \\ i \end{pmatrix}. \tag{2.23}$$

2.2.3 Eigenvectors of Jones Matrices

An eigenvector of any matrix is defined as a particular vector which, when multiplied by the matrix, gives the same vector within a constant factor, in Jones calculus this can be written:

$$\begin{pmatrix} a & b \\ c & d \end{pmatrix}. \begin{pmatrix} A \\ B \end{pmatrix} = \lambda \begin{pmatrix} A \\ B \end{pmatrix}.$$

The constant λ, which may be real or complex, is called the eigenvalue.

Physically, an eigenvector of a given Jones matrix represents a particular polarization of a wave which up on passing through the optical element in question, emerges with the same polarization as when it entered. However, depending on the value of λ, the amplitude and the phase may change. If write $\lambda = |\lambda| e^{-i\phi}$, then $|\lambda|$ is the amplitude change, and ϕ is the phase change.

The problem of finding the eigenvalues and the corresponding eigenvectors of a 2×2 matrix is quite simple. The matrix equation above can be written as:

$$\begin{pmatrix} a - \lambda & b \\ c & d - \lambda \end{pmatrix}. \begin{pmatrix} A \\ B \end{pmatrix} = 0. \tag{2.24}$$

Now in order that a nontrivial solution exists, namely one in which A and B are not both zero, the determinant of the matrix must vanish.

$$\begin{pmatrix} a - \lambda & b \\ c & d - \lambda \end{pmatrix} = 0, \tag{2.25}$$

this is a quadratic equation in λ, known as the secular equation. Up on expanding the determinant we get

$$(a-\lambda).(d-\lambda) \text{ - b c= 0.}$$

Whose roots λ_1 and λ_2 are the eigenvalues. To each root there is a corresponding eigenvector. These can be found by noting that the matrix Eq.2.24 is equivalent to the two algebraic equations i.e

$$(a-\lambda).A + bB = 0 \qquad\qquad cA + (d-\lambda).B = 0, \tag{2.26}$$

the ratio of A to B, corresponding to a given eigenvalue of λ,can be found by substitution of λ_1 and λ_2 in to either equation [10,16].

2.2.4 Jones Reflection Matrix

In the case of either internal or external reflection, one can identify the TM components as "horizontal" and the TE components as "vertical" then it can utilized the Jones calculus by defining a reflection matrix as

$$\begin{pmatrix} -\mathbf{r}_p & 0 \\ 0 & \mathbf{r}_s \end{pmatrix}. \tag{2.27}$$

The Jones vector of the reflected light is then given by

$$\begin{pmatrix} A' \\ B' \end{pmatrix} = \begin{pmatrix} -\mathbf{r}_p & 0 \\ 0 & \mathbf{r}_s \end{pmatrix} . \begin{pmatrix} A \\ B \end{pmatrix}, \tag{2.28}$$

where $\begin{pmatrix} A \\ B \end{pmatrix}$ is the vector of the incident light and $\begin{pmatrix} A' \\ B' \end{pmatrix}$ is the vector of the reflected light. The vector of $\mathbf{r}_p$ and $\mathbf{r}_s$ are given a function of the angle of incident by using Snell's law and considering Eqs.(1.72) and (1.73) i.e

$$\mathbf{r}_s = \frac{\cos\theta - \sqrt{n^2 - \sin^2\theta}}{\cos\theta + \sqrt{n^2 - \sin^2\theta}}, \tag{2.29}$$

$$\mathbf{r}_p = \frac{-n^2\cos\theta + \sqrt{n^2 - \sin^2\theta}}{n^2\cos\theta + \sqrt{n^2 - \sin^2\theta}}. \tag{2.30}$$

Here the most important point is to know that, off-diagonal elements of these matrices Eq.2.28 are zero for isotropic dielectrics and non-zero values of the off-diagonal elements can occur in the case of anisotropic substances, such as crystals. For further treatment of reflection matrix, the case of normal incidence as an example is considered. Here, the reflection matrix is given by

$$\begin{pmatrix} -\rho & 0 \\ 0 & \rho \end{pmatrix} = \rho. \begin{pmatrix} -1 & 0 \\ 0 & 1 \end{pmatrix}, \tag{2.31}$$

where $\rho = \frac{1-n}{1+n}$ and n is the relative index of refraction. Suppose that the incident light is a right circularly polarized, so that its Jones vector is $\begin{pmatrix} 1 \\ -i \end{pmatrix}$. The Jones vector of the reflected light is then

$$\rho. \begin{pmatrix} -1 & 0 \\ 0 & 1 \end{pmatrix} . \begin{pmatrix} 1 \\ -i \end{pmatrix} = \rho. \begin{pmatrix} -1 \\ -i \end{pmatrix} = \frac{n-1}{n-1}. \begin{pmatrix} 1 \\ i \end{pmatrix}. \tag{2.32}$$

Thus the reflection light is left circularly polarized, and its amplitude is changed by the factor $\frac{n-1}{n+1}$. Similarly, its found that if the incident light is left circularly polarized, then the reflected light is right circularly polarized. this reversal of the handedness of the circular polarization is independent of the value of n, and thus occurs in the case of both internal and external reflection provided the angle of incidence is small [10].

2.2.5 Stoke‘s vector

The modern representation of polarized light actually had its origins in 1852 in the work G.G.Stokes. He introduced four quantities that are functions only for observable of the electromagnetic wave and are now known as the Stokes parameters. The polarization state of a beam of light (either natural or totally or partially polarized) can be described interims of these quantities. To see it, let us specify

an ellipse with its major axis is (a), its minor axis is (b) and the angle (ϕ) the major axis makes with the x-axis:

$$b \leq a \qquad\qquad 0 \leq \phi < \pi. \tag{2.33}$$

A derived parameter, which may be called "ellipticity"

$$|\chi| = \tan^{-1}(\frac{b}{a}) \qquad\qquad \frac{-\pi}{4} \leq \chi \leq \frac{\pi}{4}, \tag{2.34}$$

is often useful.(The sign of χ indicates handedness, χ being negative for left-handed polarization). This parameter, when divided by $\frac{\pi}{4}$, is a measure of the extent to which the ellipse approaches a circle.

$\frac{4}{\pi}\ \chi$ = 0,1

corresponding, respectively, to linearly and circularly polarized light. The two sets of parameters (E_x, E_y, ψ, α) and (a, b, ϕ, χ) can be shown to be related as follow.

$$a^2 + b^2 = E_x^2 + E_y^2, \tag{2.35}$$

$$\tan 2\phi = \cos\psi \tan 2\alpha, \tag{2.36}$$

$$\tan 2\chi = \sin\psi \sin 2\alpha. \tag{2.37}$$

It may help to visualize the state of polarization by plotting the ellipse conceptually as a point on a unit sphere, called the Poincare sphere (see fig.2.4), on which the the equator corresponds to linearly polarized light and the north and south poles, respectively, to right and left circularly polarized light. More generally, the latitude:

$$\theta = 2\chi, \tag{2.38}$$

corresponds to double the "ellipticity" and the longitude:

$$\varphi = 2\phi, \tag{2.39}$$

to twice the angle of the major axis.

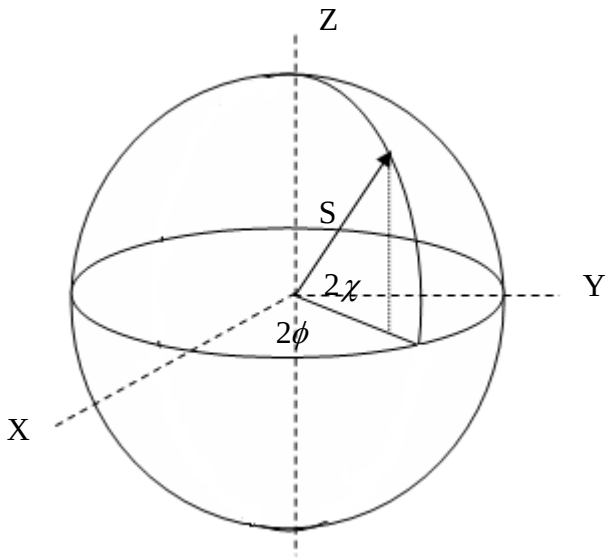

Figure 2.3: *The Poincar'e sphere.*

If information concerning the magnitude of the radiation is of interest, the radius [9], of the sphere is taken in proportion to the intensity of the wave.

Here, for the sake of convinces cartesian coordinate system is considered, so that the z-axis passe through the poles and the longitude φ is measured from the xy-plane, the ordered array

$$\begin{pmatrix} s \\ x \\ y \\ z \end{pmatrix}, \tag{2.40}$$

can be used to specify point x ,y ,z on Poincar'e sphere. it is the Stokes vector of the state of polarization corresponding to the point x ,y ,z. for fully polarized light

$$x^2 + y^2 + z^2 = s^2. \tag{2.41}$$

In terms of the two sets of parameters by which we have described the state of polarization:

$$s = a^2 + b^2 = E_x^2 + E_y^2, \tag{2.42}$$

$$x = s\cos 2\chi \cos\phi = E_x^2 - E_y^2, \tag{2.43}$$

$$y = s\cos 2\chi \sin\phi = 2E_x E_y \cos\psi, \tag{2.44}$$

$$z = s\sin 2\chi = 2E_x E_y \sin\psi. \tag{2.45}$$

In each case the first equality follows readily from the geometry in fig.2.3 and the second equality can be derived there from by means of Eqs.(2.1) and (2.34) to (2.37).

For unit intensity, linearly polarized light the stokes vector has the form

$$\begin{pmatrix} 1 \\ \cos 2\alpha \\ \sin 2\alpha \\ 0 \end{pmatrix}, \tag{2.46}$$

and for right and left circularly polarized light

$$\begin{pmatrix} 1 \\ 0 \\ 0 \\ \pm 1 \end{pmatrix}, \tag{2.47}$$

respectively [14,15]. In this experiment, since polarized light is used, Jones matrices may applied frequently throughout this paper.

Chapter 3

THEORY AND MEASUREMENTS OF RAS

3.1 Introduction

In this chapter the basic principles of the optical technique RAS and its application in the study of the optical property of surfaces described. The field of surface science has changed dramatically with the discovery of Scanning Tunnelling Microscopy (STM) by Binnig and Rohrer, in 1983 [17]. Since then, it has become possible to image almost routinely surfaces and surface bound species with atomic scale resolution. The STM has allowed to visualized quantum mechanics as never before.

The surface of solid is inherently different than the rest of the solid (bulk), specially in the case of their bonding properties. Surface atoms simply cannot satisfy their bonding requirements in the same way as bulk atoms. Therefore, surface atoms will always want to react in some way, either with each other or with foreign atoms to satisfy their bonding requirement [17]. When light reflected from the surface of material it contains information about the nature of the surface [18].

More recently, a variety of ways have been devised for directly measuring surface effects in optical reflectivity. For instant, in surface differential reflectivity

(SDR) technique, the incident light is split (in time, using a chopper) between two identical samples, one of which is modified, for example by adsorption. Here, the ratio $\frac{I_\omega}{I_0}$ is the value required which is directly proportional to $\frac{\Delta R}{R}$, the fractional difference is ratiometric, and it is surface specific. SDR provided the first conclusive demonstration of the use of reflectivity spectra in the detection of surface states. The technique, however, is not applicable if a reference surface is not available.

An alternative approach to surface specificity is the symmetry, as exemplified by Second Harmonic Generation (SHG). While centro-symmetric materials have null second order polarizability, this symmetry is necessarily broken at a surface. Thus second order reflection (i.e. light reflected with two times the frequency of the incident light), derived specifically from the surface and this method becomes increasingly important in surface studies.

Recently Beleckman et al have proposed a new reflection spectroscopy which is surface specific without imposing symmetry constrains on the surface [19]. This technique known as 45 degree reflectometry (45DR), relies on a particular feature of the Fersonal equations. At 45^0 angle of incident, for a mathematically sharp and clean interface, R_S^2 is identical to R_P irrespective of the dielectric constants of material. Measuring the quantity Δ_{45} = $R_S^2(45^0)$ - $R_P(45^0)$ thus allows one to detect directly any deviation from the ideal sharp, clean interface and to study its properties. The sharp interface assumed in Fresnels equations is a mathematical model, real systems are characterized by a transition region can thus in principle be studied by measuring the difference between $R_S^2(45^0)$ and $R_P(45^0$.

The surface sensitivity of this Δ_{45} technique is in general not as high as that of ellipsometry, since the optimum angle for ellipsometry is close to the pseudo Brewster angle, and for metals and semiconductors the pseudo Brewster angle is well above 45^0. However, the built in baseline allows one to do direct measurements of, for example, the surface states, surface roughness and so on, without resorting to a ”before-after” strategy.

Spectroscopic ellipsometry (SE) is another ratiometric modulation technique. In this case the sample is not modified, but rather the polarization of the incident

light is modulated between the perpendicular and horizontal states, and $\frac{r_p}{r_s}$ is measured. (r represent complex Fersnel reflection amplitudes and are related to the corresponding reflectivities, R, by $R =\mid r \mid^2$) [20,21,22].

Generally, optical spectroscopy is extensively used to characterize surfaces, the dominating techniques being reflectance anisotropy spectroscopy (RAS) and spectroscopic ellipsometry (SE) [20]. Already in 1966 Cardona et al observed that rotating a Si(110) sample around the surface normal changed the reflectivity as a function the azimuthal angle. However, it took about twenty years before the phenomenon of surface-induced optical anisotropic started to be investigated systematically. The high potential of RAS for growth-monitoring was demonstrated by Kamiya et al [24]. By measurements on GaAs(001) in ultra-high vacuum as well as in atmospheric pressure of H_2, He and N_2. It was noted that each of the well-known GaAs(001) surface reconstructions such as (4×4), (2×4) and (4×2) gives rise to a characteristic, fingerprint-like RAS spectrum. The correlation between reflection high-energy electron diffraction patterns and the RAS spectra allowed them to establish a database for GaAs(001) surface reconstruction.

The surface reconstruction can thus be determined in-situ, even at ambient conditions. For many semiconductors a change of the surface reconstruction during layer growth occurs. RAS can, therefore be easily used to monitor growth and layer completion. This application has proven highly successful and is now exploited commercially. However, surface optical spectroscopic gives only indirect information about the surface structure and chemistry. The intuitive interpretation of the spectra in terms of bond polarizabilities is difficult and often leads to wrong results even for relatively simple surfaces. Reliable calculations of surface optical spectra are needed to fully exploit their diagnostic potential.

One of the first major attempts to calculate surface optical properties was made by McIntyre and Aspens [23,25,26]. They approximated the inhomogeneity of the surface dielectric tensor by a two-step function, i.e. modeled the surface by three-layer system consisting of vacuum, thin film and substrate. This model was later extended to include surface anisotropy and remains very popular because of its simplicity. A more general approach was take in 1979 by Bagchi et al. They

started by considering a semi-infinite electron gas. The truncation of the bulk leads to modification of the optical properties in the surface region. Based on the assumption that this region is much thinner than the light wave-length, the light propagation equations were solved. A few years later Del Sole generalized this model to the case of larger anisotropic in real crystal and obtained an expression for the surface contribution to the reflectance, $\frac{\Delta R}{R}$, where R is the reflectance according to the Fresnel equation [26].

Since the first studies on the cleavage surfaces of Si and Ge, reflection spectroscopy has proven to be a powerful probe of surface electronic properties. In those studies, the fundamental problem of discriminating between optical transitions of different origin of identifying surface-related structures against bulk feature was addressed by direct composition between the experimental spectra obtained for the clean and chemisorbed surfaces [differential reflection (DR) spectroscopy]. More recently an alternative approach to this problem, based on the study of reflectance anisotropic (RA), has been introduced.

Both methods, however, are indirect, as both chemisorption-induced modifications of the optical properties and intrinsic anisotropic of clean surfaces cannot always be directly attributed to electronic transitions involving surface states. Indeed, the effect of chemisorption may be much more complex than the pure quenching of clean surface states: new states may arise, and those of the clean surface may still be present, with modified energies and wave functions. Similarly, the origin of anisotropic in surface optical properties cannot always be attributed to anisotropic in the spectrum of surface state, since they occur even at natural surfaces, where no optically active surface state is expected in the frequency range of interest.

For Si(111) 2×1, the simple interpretation of DR data in terms of transitions between surface states was still able to provide a great amount of information, because in this case the main surface-related optical features correspond to below-band-gap transitions. For the higher energy features of the DR spectrum, however, calculations of surface optical properties based on a semiempirical tight-binding approach have shown that above-band-gap DR features are not directly

related to surface state, owing to a strong geometrical effect induced on bulk states by reconstruction.

Starting to the first published work on RDS/RAS technique, there has been a rapid growth of the field, as can be seen in the scientific literature. The number of publication in peer-reviewed journals from 1987 to 2004 inclusive involving RAS is shown in fig.3.1.

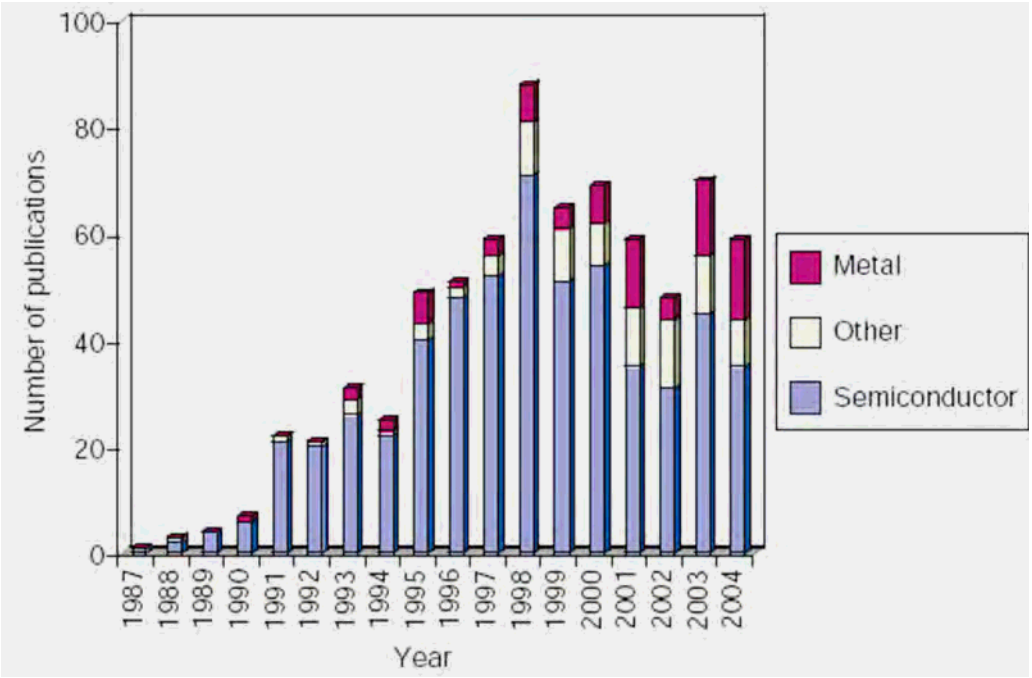

Figure 3.1: *Historical growth of RAS.*

The publications have been categorized broadly in to research involving semiconductors, metals or others systems. The figure shows that RAS associated with semiconductors research has dominated the field. However, the technique has provide to be very versatile and has recently been applied electrochemical environments [23].

In this work RAS technique is applied for investigating surface properties, since RAS takes advantage of the anisotropy found in surface reconstructions to obtain a very high surface sensitivity. Anisotropy in the optical response is

common to many materials of current interest. Super-lattices, whether semiconduction or metallic, are optically anisotropic and can be represented by a set of uniaxial optical constants with optical axis normal to the surface [20].

RAS is a powerful tool for characterizing the surface of crystalline materials and initially it was applied to semiconductor surfaces as mentioned above. The measurement of RAS requires an accurate method of determining the polarization state of light reflected from clean and smooth surface. In RAS method the spectroscopic range from near IR through visible to near UV part of the spectrum (1-6 ev) is utilized.

In most cases, RAS technique is employed to probe the anisotropy of single crystal surfaces. Advances in the interpretation of reflectance spectroscopy spectra are made possible by the understanding of the reflectance spectroscopy response from clean surface prepared in Ultra-high vacuum environment. Such studies benefit from the availability of a wide range of probes to characterize the surface such as scanning tunnelling microscope, low energy electron diffraction (LEED), X-ray photoelectron spectroscopy (XPS), ultra- violet photoemission (PE) and inverse photoemission (IPE) spectroscopy. Combining these techniques with RAS provides insight in to the atomic and electronic structure and the morphology of surface [23,27].

The physical origin of the reflectance anisotropy has been attributed to contributions from transitions between surface and bulk electronic states [28], anisotropy in the surface region. Because, the surface has lower symmetry than the bulk and bulk spatial dispersion, microscopic and macroscopic roughness [24,29,30,31]. Also, the difference of the dielectric response along and perpendicular to the optical axis may be responsible for the origin of RAS signals [23].

3.2 Principles and Instrumentations of Reflectance Anisotropic Spectroscopic

3.2.1 Basic optical principles of RAS

Optical spectroscopies are extremely valuable for the in-situ, non-destructive and real-time surface monitoring under challenging conditions as may be encountered, eg. during epitaxial growth. RAS is one of the plethora of surface sensitive spectroscopies probing linear optical coefficients, which has been particularly successful in exploring surface structures [23,32].

Reflectance anisotropy spectroscopy, also termed reflectance difference spectroscopy (RDS) [24,33] measures the relative difference in complex reflection coefficients $\frac{\Delta r}{r}$ for light polarized along two perpendicular directions within the sample surface plane; normalized to the average reflectance r [25,27,34].

$$\frac{\Delta r}{r} = 2\frac{r_x - r_y}{r_x + r_y} = Re(\frac{\Delta r}{r}) + iIm(\frac{\Delta r}{r}) \tag{3.1}$$

Where r_x and r_y are complex Fresnel reflectances of light polarized linearly along the indicated directions within the surface [15,21,25,27]. Here, the relative difference $\frac{\Delta r}{r}$ in complex reflectances, which can be related to the relative (power) reflectance difference is given as:

$$\frac{\Delta R}{R} = \frac{R_x - R_y}{R},$$

according to

$$\frac{\Delta R}{R} = 2Re(\frac{\Delta r}{r}), \tag{3.2}$$

Where $R_x = \mid r_x \mid^2$ etc [29,33,35] and R is the average value $\frac{R_x - R_y}{2}$. Note that $\frac{R_x - R_y}{R}$ is just the normalized peak-to-peak value of the sinusoidal component of the detected beam [36]. However, residual linear polarization of the source and residual linear polarization sensitivity of the detector may affect the result [31,37]. Of course baseline correction can be achieved by taking the polarizing axis oriented $+45^0$ and -45^0 relative to the optical axis [28,32]. The signals to be detected are usually of the order of $\mid \frac{\Delta r}{r} \mid = 0.001 - 0.01$ and carry information originating

only from the surface region because the bulk beneath is optically isotropic and therefore does not contribute to the measured spectrum [23,25,27].

3.2.2 Intensity Modulation

If we are considering linearly polarized light at near-normal incident on a sample rotating with angular frequency ω in the diagonal frame of the sample, the time-dependent polarization vector of the input light has the form $\begin{pmatrix} sin\omega t \\ cos\omega t \end{pmatrix}$. The intensity of the light reflected by the sample is therefore

$$I \sim R - \frac{\Delta R}{2}\cos 2\omega t, \tag{3.3}$$

where R and ΔR represent, respectively, the average and the anisotropy of the reflected intensities, hence, both of them can be expressed interims of r_x and r_y in the following ways.

$$R = \frac{\mid r_x \mid^2 + \mid r_y \mid^2}{2} \qquad\qquad \Delta R = \mid r_x \mid^2 - \mid r_y \mid^2 \tag{3.4}$$

The ratio of the oscillatory $(I_{2\omega})$ and time-independent (I_0) intensities contributions to the reflected intensity is a direct measurement of $\frac{\Delta R}{R}$:

$$\frac{I_{2\omega}}{I_0} = \frac{1}{2\sqrt{2}}\frac{\Delta R}{R}, \tag{3.5}$$

or

$$\frac{\Delta R}{R} = 2\sqrt{2}\frac{I_{2\omega}}{I_0}. \tag{3.6}$$

The RAS signal $\frac{\Delta R}{R}$ and conventional reflectance signal R can be easily separated by using frequency selective and phase selective amplifiers in the detection system. The main disadvantage of the rotating sample spectrometry is simply that it is not always convenient or even possible to rotate the sample, particularly for in-situ studies. The remedy would appear to be trivial: rotate the polarizer in steady of the sample.

An inherent drawback with mechanically rotating components is the difficulty

of maintaining precise alignment. In addition, mechanical modulation techniques are relatively slow since a signal modulation cycle is usually of the order $\geq 10^{-2}$ sec [23,30].

3.2.3 Phase Modulation

As in related fields, photoelastic modulation has became popular in the RAS community. The photoelastic modulation (PEM) is essentially a dynamic wave plate. In effect, one linearly polarization, perpendicular to the modulation axis, is unaffected by the PEM, while light polarized along the modulation axis undergoes a retardation, Γ, which can be given by:

$$\Gamma = \Gamma_0 \sin(\omega t) \tag{3.7}$$

To achieve significant retardation (we will see that Γ_0 approaching half wave retardation is required) the crystal must be driven at its resonance frequency. Since the speed of sound in crystals is of the order of 10^3, resonant frequencies are of the order of 10^5 Hz for devices with physical dimensions of the order of 10^{-2} m. In addition to high speed and low noise, PEM modulation offers greater information content than the intensity modulating techniques discussed above. RAS is most fully expressed as $\frac{\Delta r}{r}$, a complex quantity, while $\frac{\Delta R}{R}$ is real and, for small anisotropies, approximately equal to $2Re(\frac{\Delta r}{r})$. By modulating phase rather than intensity, measurement of both the real and imaginary parts of $\frac{\Delta r}{r}$ becomes possible.

The standard phase modulating reflectance anisotropic spectrometry has three polarization-sensitive elements, i.e, a polarizer, PEM and an analyzer when the last two elements are placed after reflection of light from the sample. The transmission axes of the polarizer and PEM are parallel but the transmission axes of the an analyzer is making 45^0 from the transmission axis of PEM. The electric amplitude of the light reaching the RAS detector is described by the expression:

$$A \sim \begin{pmatrix} 1 & 0 \\ 0 & 0 \end{pmatrix} \begin{pmatrix} cos(\frac{\Gamma}{2}) & isin(\frac{\Gamma}{2}) \\ isin(\frac{\Gamma}{2}) & cos(\frac{\Gamma}{2}) \end{pmatrix} \begin{pmatrix} r_x & 0 \\ 0 & r_y \end{pmatrix} \begin{pmatrix} 1 \\ 1 \end{pmatrix}, \tag{3.8}$$

and it follows that I, the light intensity reaching the detector, is a harmonic series $I_0 + I_\omega + I_{2\omega} + ...$ where I_0 is time-independent and the remaining terms are root-mean-square oscillations at the angular frequencies indicated by the subscripts. Setting Γ_0 to 2.405 radians ensures $J_0(\Gamma_0) = 0$, where J_n is a Bessel function of order n, and leads to

$$\frac{I_{n\omega}}{I_0} = 8\frac{J_n(\Gamma_0)Im(\frac{\Delta r}{r})}{4+ \mid \frac{\Delta r}{r} \mid^2} \approx 2J_n(\Gamma_0)Im(\frac{\Delta r}{r}), \tag{3.9}$$

where n is an odd integer, and

$$\frac{I_{n\omega}}{I_0} = 8\frac{J_n(\Gamma_0)Re(\frac{\Delta r}{r})}{4+ \mid \frac{\Delta r}{r} \mid^2} \approx 2J_n(\Gamma_0)Re(\frac{\Delta r}{r}), \tag{3.10}$$

Where n is an even integer. Generally standard analogue lock-in amplifiers are used to measure the fundamental and first harmonic (and hence determine $\frac{\Delta r}{r}$), but digital lock-in amplifiers of extinction ratio of the order of 10^5 s. have been successfully employed to measure higher order harmonics, enabling high speed measurements. In principle, the phase modulating RA spectrometry eliminates mechanically derived noise but is sensitive to other instrumental errors that are tolerated by the rotating analyzer and rotating sample spectrometry [23,25].

3.3 Crystal Symmetry and Anisotropy

A mineral is a naturally occurring homogeneous solid with a definite (but not generally fixed) chemical composition and a highly ordered atomic arrangement, usually formed by an inorganic process. That is, atoms in a mineral are arranged in an ordered geometric pattern. This ordered arrangement is called a *crystal structure*, and thus all minerals are crystals. For example, every crystal of quartz will have the same ordered internal arrangement of atoms. A solid compound that meets other criteria, but has not definite crystal structure is said to be *amorphous*. In all crystals angles between corresponding crystal faces of the same mineral have the same angle. This is true even if the crystal faces are distorted (Steno's law).

One of the consequences of this ordered internal arrangement of atoms is that all crystals of the same mineral look similar and it is believed that crystals are formed by a regular repetition of identical building blocks. When a crystal grows in a constant environment the shape remains unchanged during growth, as if identical building blocks are added continuously to the crystal. That mean it is possible to describe the structure of all crystals in terms of a single periodic lattice, but with a group of atoms attached to each lattice point or situated in each elementary parallelopiped. This group of atoms is said the basis; the basis is repeated in space to form the crystal.

Crystals have an ordered internal arrangement of atoms, i.e., atoms are arranged in a symmetrical fashion on a three-dimensional network referred to as lattice. The crystal faces reflect the ordered internal arrangement of atoms and thus reflect the symmetry of the crystal lattice. Analysis of the internal motion of a crystal relies heavily upon the symmetry properties of the crystal. Crystal may be symmetrical with relation to planes, axes and centers of symmetry. Planes of symmetry divide crystals in to equal parts (mirror image) that correspond point for point, angle for angle and face for face. In the case of symmetry with respect to an axis (Rotational symmetry), an axis is an n-fold axis of symmetry, if for every point of the object, **p**, there is a corresponding point **p'** on the plane perpendicular to the axis and at equal distance from the axis, but rotated by an angle $\frac{2\pi}{n}$ about the axis. An n-fold rotation symmetry is defined as an operation with a minimum rotation angle of $\frac{2\pi}{n}$; only 2-fold, 3-fold, 4-fold and 6-fold rotations may occur among the symmetry operations of a crystal lattice.

An object that requires rotation of a full 360^0 in order to restore its original appearance has no rotational symmetry. Since it repeats itself one time every 360^0 it is said to have a 1-fold axis of rotational symmetry. Thus 1-fold symmetry implies no symmetry at all and this condition can also one characteristic of isotropy crystals. If an object appears identical after a rotation of 180^0, that is twice in a 360^0 rotation, then it is said to have a 2-fold rotation axis, most of the time this phenomenon is observed in anisotropic crystals. For the case of 3-fold rotation axis an objects repeat themselves three time in a 360^0 rotation. Although objects

themselves may appear to 4-fold, 5-fold, 6-fold, 7-fold and 8-fold or higher-fold rotation axes, there are not possible in crystals. The reason for this is that the external shape of crystal is based on a geometric arrangement of atoms. Note that if one try to combine objects with 5-fold and 8-fold apparent symmetry, it is impossible to combine them in such a way that they completely fill space. Note also in the context of axis of symmetry that a 4-axis is also a 2-axis and a 6-axis is also 2- and 3-axis. Where 1, 2, 3, 4 and 6 fold axes are also called the *proper axis*. A rotation operation and inversion about a center of symmetry on the axis leaving the object unchanged, mean the axis is *improper axis*. An improper n axis of symmetry is defined by $\overline{n}$. Therefore, as one have 1, 2, 3, 4 and 6 axes, it is also possible to have $\overline{1}$, $\overline{2}$, $\overline{3}$, $\overline{4}$, $\overline{6}$ axes as the the equivalent improper axes. Here note that, $\overline{1}$ is simply a center of symmetry, $\overline{2}$ gives a mirror image about the plan m, perpendicular to $\overline{2}$ axis through the axis of symmetry. $\overline{2}$ axis usually denoted by its plan m and $\overline{3}$-fold axis is also a 3-fold axis and with a center of symmetry on the axis. Therefore, all the symmetries with respect to a plan, a line and point can now be classified in to 10 basic symmetry elements i.e. 1, $\overline{1}$, 2, m, 4, $\overline{4}$, 3, $\overline{3}$, 6, $\overline{6}$. Again if a point on a 2, 4, 6 fold axis is a center of symmetry, then the plane perpendicular to the axis through the center of symmetry is a mirror plane thus, the combination will be expressed as $\frac{2}{m}$, $\frac{4}{m}$, or $\frac{6}{m}$. Thus one can obtain 13 groups of single axis of symmetry which are given as 1, $\overline{1}$, 2, m, $\frac{2}{m}$, 4, $\overline{4}$, $\frac{4}{m}$, 3, $\overline{3}$, 6, $\overline{6}$, $\frac{4}{m}$. Intersecting of proper axes of symmetry are characterized by 2 2 2, 3 2 2, 4 2 2, 6 2 2, 2 3 3, 4 3 2 and adding center of symmetry to each given six new groups one may have $\frac{2}{m}\ \frac{2}{m}\ \frac{2}{m}$, $\overline{3}\ \frac{2}{m}\ \frac{2}{m}$, $\frac{4}{m}\ \frac{2}{m}\ \frac{2}{m}$, $\frac{6}{m}\ \frac{2}{m}\ \frac{2}{m}$, $\frac{2}{m}\ \overline{3}\ \overline{3}$ and $\frac{4}{m}\ \overline{3}\ \frac{2}{m}$ in addition by replacing two of these even folded axes to give 7 new compatible sets of compatible proper and improper axes. Thus by considering the above all type of symmetry they display crystallin substances are grouped in to 32 classes. These in turn are grouped in to seven systems on the basis of the relation ships of their axes, i.e, imaginary straight lines passing through the ideal centers of the crystal. These basic groups can be classified in to the following crystal classes:

From the basic formula for generator matrices, one can define the generator matrices for each of these classes. Once the generator matrices are found, it is

Triclinic	$1, \bar{1}$
Monoclinic	2, m, $2/m$
Orthorhombic	2 2 2, 2 m m, $2/m\ 2/m\ 2/m$
Tetragonal	$4, \bar{4}, 4/m$, 4 2 2, 4 m m, $\bar{4}$ 2 m, $4/m\ 2/m\ 2/m$
Cubic	2 3 3, 4 3 2, $\bar{4}$ 3 m, $2/m\ \bar{3}\ \bar{3}$, $4/m\ \bar{3}\ 2/m$
Trigonal	3, $\bar{3}$, 3 2 2, 3 m m, $\bar{3}\ 2/m\ 2/m$
Hexagonal	6, $\bar{6}$, $6/m$, 6 2 2, 6 m m, $\bar{6}$ 2 m, $6/m\ 2/m\ 2/m$

Table 3.1: *The seven crystal systems.*

easily to define the bond matrices for each class and hence the elastic coefficient matrix for each class. Thus, in general, the lass the symmetry of a class the more is the anisotropy, which means, for higher-fold rotation axes, the crystal will not show anisotropy property [1,38,39].

3.4 Methodology

The schematic set-up of RAS spectrometry is shown in fig.3.1. Here, a well-collimated beam of monochromatic linearly polarized light from a 5 mV HeNe laser source (PHYWE), is passes through quarter-wave plate (QWP), chopper and polarizer (P) section of the instrument. The model SR540 optical chopper is used to square-wave modulate the intensity of optical signals. The unit can chop light sources at rates from 4 HZ to 3.7 KHZ. The light emergent from the polarizer is reflected at near-normal incidence ($\approx 5^0$ off normal) from the specular surface of a rotating sample under study. Of course, the data reported here optend by rotating the sample at two points on the surface of the sample by using suitable stepper motor (model number 17BSC 002) which is under computer control. To do so, it has been rotated the sample $+45^0$ and -45^0 from the optical axis of the studied optical material (determination of optical axis will be discussed in the

next chapter). In this experiment, since the interest is only on the light coming along and perpendicular to the optical axis, the reflected light must passe through analyzing section of the instrument that consists analyzer (A) its, transmission axis is making 45^0 that of polarizer, followed by a photodetector (D). The detector detects the light flux affected the light has travelled through the polarizer-analyzer sequences of elements. Thus the light received by the photodetector is amplified for measurement by a lock-in amplifier (LIA) (Stanford research systems, model SR830 DSP). Since LIA is interfaced with the computer having a LabView software, the data will be easily accessed.

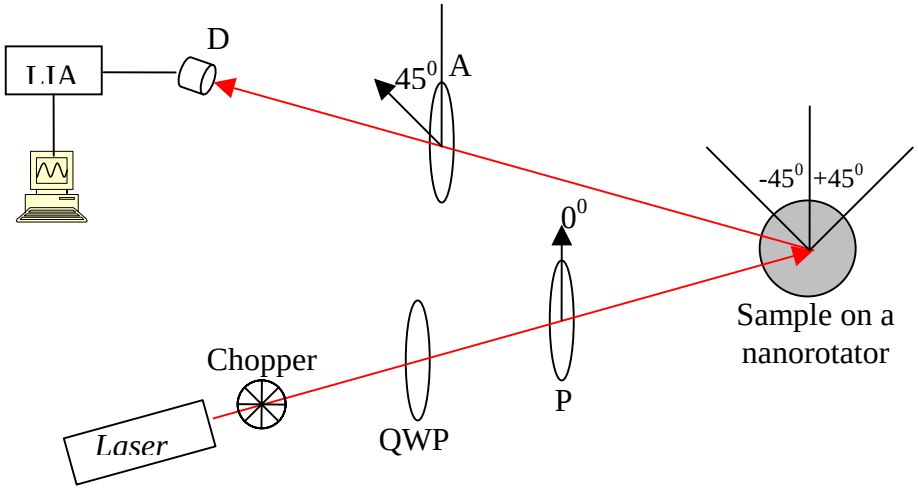

Figure 3.2: *Schematic diagram of RAS.*

Chapter 4

Data Analysis and Interpretation

4.1 Determination 0f Optical Axis 0f KTP Crystal

As discussed in the previous chapters, to apply the optical technique RAS it is mandatory first to determine the optical axis of the sample under study. Here, the main question is how to determine the optical axis of the sample? Before determining the optical axis, it is necessary to investigate the properties of transmitted and reflected light along the optical axis of a material having optical axis. As it has been seen in section 1.2.2 by considering 3-Dimension. $\overrightarrow{k}$ space, when light of arbitrary polarization propagates through anisotropic crystal, it can be considered to consist two independent waves that are polarized orthogonally with one other and travelling with different phase velocities. But those two phase velocities may have the same value, when they are propagating in the direction of an optical axis of the crystal see fig.1.3. Similarly, one may expect that the light reflected from the optical axis may have also some peculiar characteristic. To see this spacial nature of the reflected light the well-known KTP crystal was taken. It is known that KTP is a biaxial crystal and has three principal refractive indices, n_1, n_2 and n_3 which are all different in magnitude [2]. Since KTP is anisotropic crystal it has crystallographically distinct axes and interact with light by a mechanism that is dependent upon the orientation of the crystallin lattice with respect

to the incident light angle. When light enters the optical axis of anisotropic crystals, it behaves in a manner similar to the interaction with isotropic crystal, and passing through at a single velocity. However, when light enters a non-equivalent axis, it is refracted into two rays each polarized with vibration directions oriented at right angles to one another, and travelling at different velocities. From this phenomenon one can easily realize that, the intensity of transmitted light along the optical axis is some what intense than the reflected light from the optical axis. Keeping this in mind, it was considered to be necessary to investigate the property of the reflected light from the two optical axes of the crystal. The experimental set-up used is shown in fig.3.2. Care was taken, so that the HeNe laser light be incident, as much as possible, at the center of the well-polished KTP crystal, i.e. the reflected light from the crystal should be on the same point when the sample rotate 360^0. After the above two important and tedious procedures were performed, the experiment was carried out. The data collected is shown in fig.4.1.

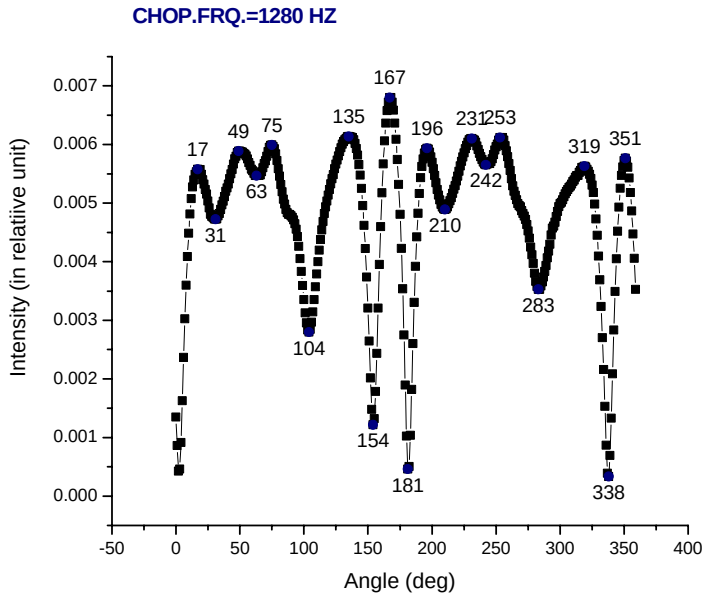

Figure 4.1: *Reflected light as a function of the angle of rotation of KTP crystal.*

As it has been discussed in section 3.3, for a system under consideration

is said to be anisotropy, it must have at least one 2-fold rotation axis (one c_2 symmetry elements) and absence of higher order symmetry like 4-fold, etc rotation axes. From fig.4.1, the intensities at 0^0, 154^0, 181^0 and 338^0 represents minimum values. Compering the pair of angles 0^0 and 181^0 and 154^0 and 338^0 the difference in the pair of angles, considering the accuracy of the experiment, is approximately 180^0. In addition the intensity of the pair of angles are nearly the same. From this one can easily observe that the crystal shows identical properties after a rotation of 180^0 in a 360^0 rotation. So, it is possible to realized that the crystal has two 2-fold rotation axes and denoted them by c_2' and c_2'', i.e., anisotropy is expressed twice. Further more, it is expected that the intensity of the reflected light from the optical axis may have minimum value comparing to the intensity of reflected light from other parts of the material. By considering the above argument the two

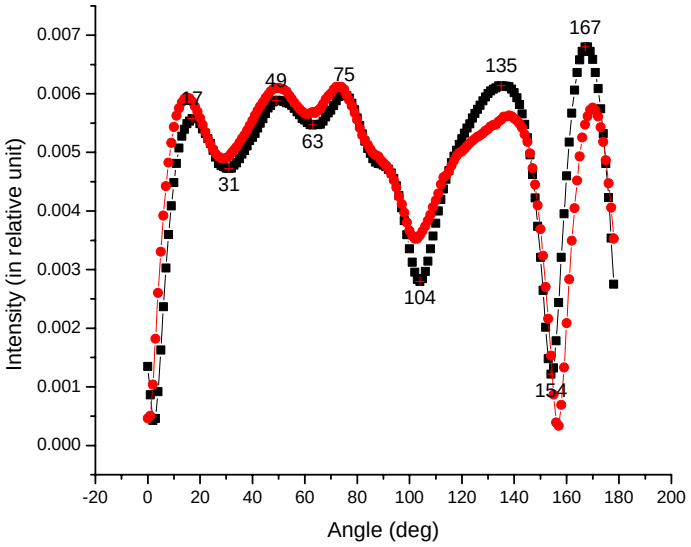

Figure 4.2: *Symmetry along* 181^0,*where G represent the values of intensities from* 182^0 *to* 360^0 .

optical axes of KTP crystal may found nearly along 154^0 and 181^0. Since for RAS technique it is enough to consider only one optical axis, therefore, it was taken the optical axis along 181^0 since the symmetry effect can be properly visualized.

Here it can be also realized that, how much the selected optical axis is symmetry by considering fig.4.2, which is shows that fitting of the values of intensity from 0^0 to 181^0 with the values of intensity from 182^0 to 360^0.

4.2 Data analysis and Interpretation

Since the optical axes of KTP crystal determined to be along 154^0 and 181^0, it is possible to calculate the degree of anisotropy by using intensity modulation method. To do so, the polarization of the incident light was adjusted in such a way that it is parallel to the selected optical axis of the crystal. Then the crystal was rotated 360^0 to take those two important parameters i.e., the reflected intensity of light along the optical axis (r_x) which is found when the optical axis make $+45^0$ from the incident light and the reflected light perpendicular to the optical axis (r_y) which is found when the optical axis make -45^0 (315^0) from the incident light see fig.4.3.

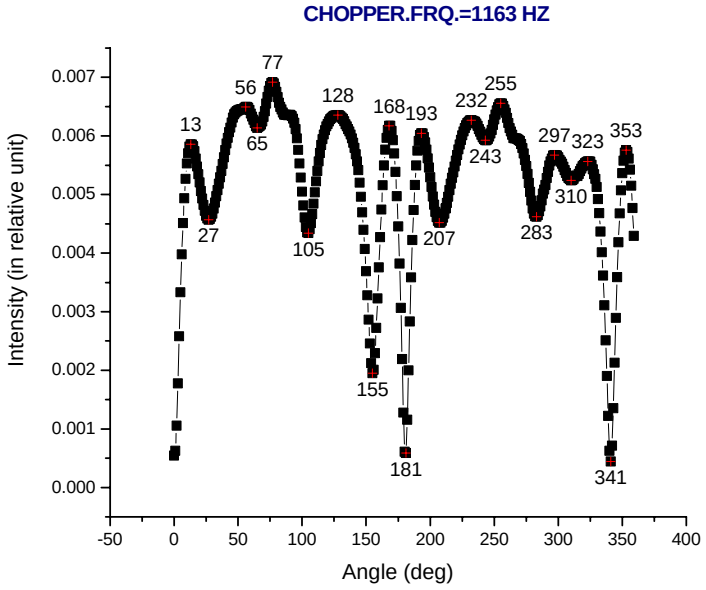

Figure 4.3: *Intensity vs angle along* 181^0 *for KTP crystal .*

The values obtained for r_x and r_y are summarized in table.4.1.

Degree	$\|r_x\|^2$	Degree	$\|r_y\|^2$
44^0	0.00614	314^0	0.00532
45^0	0.00623	315^0	0.00532
46^0	0.00631	316^0	0.00532

Table 4.1: *Values of r_x and r_y.*

Using Eq.(3.4) the degree of anisotropy of KTP crystal is computed. For the case of 44^0 and 314^0 the change in reflectance $\triangle R$ and average value of reflectance R are found to be 0.0054 and 0.15134 respectively. From the values of $(\triangle R)$ and $(\triangle R)$, the degree of anisotropy of KTP crystal is obtained to be 3.568×10^{-2}. This value is computed simply by taking the ratio of difference in reflectance and the mean reflectance. For the case of 45^0 and 315^0 the degree of anisotropy of KTP crystal is calculated to be 3.95×10^{-2}. In similar manner the degree of anisotropy of KTP crystal for the case of 46^0 and 316 is 4.12×10^{-2}. Finally by taking the results of the above three cases, the average degree of anisotropy of KTP crystal has been obtained to be 3.88×10^{-2} ± 0.00165. This results are in the range of the expected value [25,27].

In addition, from this experiment it is also possible to get the minimum as well as maximum angles between the two optical axes of KTP crystal. To do so, the sample was rotated for 720^0. The data obtained from the measurement is shown in fig.4.4. From the previous discussion it is clear that the intensity of reflected light from the optical axis is minimum. Thus from this figure it is possible to observe that, the minimum intensities of reflected light pointed at 159^0, 185^0, 340^0, 366^0, 524^0, 549^0 and 677^0. Here for the sake of simplicity the first four points were considered and one can easily realized that along which angles the two optical axes of KTP crystal is expected by considering fig.4.4.

In order to obtain those optical axes, the most important point is to represent the minimum intensities of fig.4.4 on the diagonal interception of the biaxial

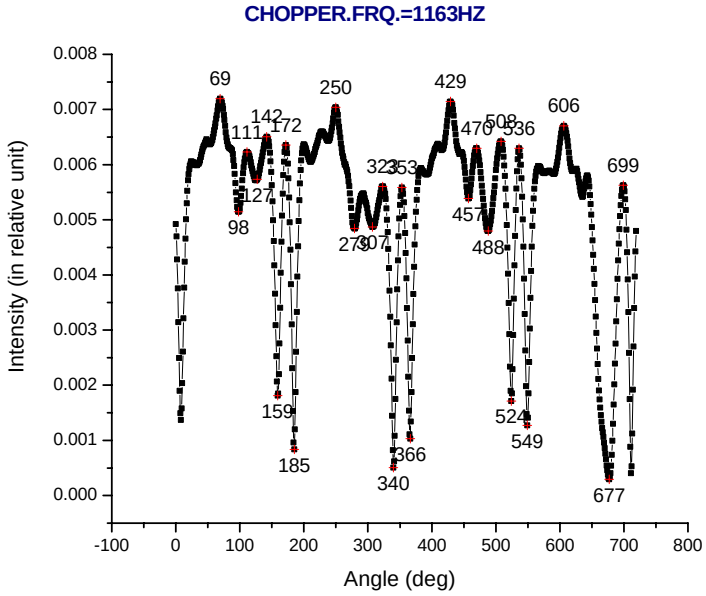

Figure 4.4: *Intensity vs angle of KTP crystal along* 181^0 *for* 720^0 .

crystal. To make it so, light of arbitrary polarization was consider, which is propagating through anisotropic crystal like KTP. The light then may be considered to consist of two independent waves (one is represented by elliptical waves and the other one is circular waves) that are polarized orthogonally with respect to each other and travelling with different phase velocities. However, there are points where the two waves touch one another. A line passing through the center and the point, where the two waves overlap, defines an optical axis. Along the axis the phase velocities of the two orthogonally polarized waves are invariant. Therefore, the above situation can be figure out in fig.4.5. From fig.4.5 it can be realized that the minimum angles between the two optical axes determined by calculating the difference between 185^0 and 159^0 or 366^0 and 340 i.e

$$\Delta\theta_1 = 185^0 - 159^0 = 26^0 \qquad or \qquad \Delta\theta_2 = 366^0 - 340^0 = 26^0, \tag{4.1}$$

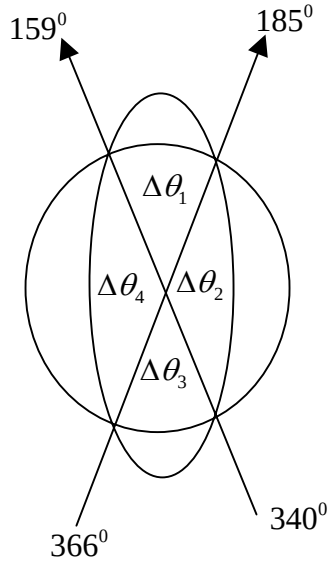

Figure 4.5: *Representation of the minimum intensities of fig.4.4.*

and the maximum angle between the two optical axes which is given by

$$\Delta\theta_3 = 340^0 - 185^0 = 155^0 \qquad \Delta\theta_4 = 366^0 - 159^0 = 157^0. \tag{4.2}$$

Since from the geometrical point of view $\Delta\theta_1 = \Delta\theta_2$ and $\Delta\theta_3 = \Delta\theta_4$, then the average of the two angle differences for the smaller separation $\Delta\theta_s$:

$$\Delta\theta_s = \frac{\Delta\theta_1 + \Delta\theta_2}{2} = 26^0.0000 \pm 0.0016, \tag{4.3}$$

and for bigger separation $\Delta\theta_b$:

$$\Delta\theta_b = \frac{\Delta\theta_3 + \Delta\theta_4}{2} = 156^0.0000 \pm 0.0017 \tag{4.4}$$

Therefore, from the results one can easily understand that how far the results are in a good agrement with the expected value. Here what is expected that,when light reflected from an optical axis of the crystal, the same properties must be observed on intensity verse angle graph after 180^0, when the crystal rotate 360^0.

4.3 RAS for the case of Basalt rock

In this section the optical technique RAS is applied to determine the degree of anisotropy of the natural basalt rock. Basalt is a hard, dense, dark volcanic rock composed chiefly of plagioclase, pyroxene and olivine, and often having a glassy appearance. The name basalt is usually given to a wide variety of dark-brown to black volcanic rocks, which form when molten lava from deep in the earth's curst rises up and solidifies. Basalt deposits frequently cover areas on many thousands of square kilometers. In general basalts are what cover all of the ocean floor and some continental areas where there is rifting as in the Ertal' Ale reagin eastern part of Ethiopia [40,41,42]. Basalt differs from granite in being a fine-grained extrusive rock and having a higher content of Iron and Magnesium. The density of basalt rock is between 2.8 and 2.9 gcm^{-3}. It is also extremely hardness 5 to 9 on Mho's scale. This gives basalt a superior abrasion resistance and casted basalt is often used as a paving and building material. Common mineral types including quartz, feldspar and biotite are often found in a glassy matrix. In general the composition in the rock is tabulated in table[4.2] as follow.

Element	SiO_2	Al_2O_3	Fe_2O_3	MgO	CaO	Na_2O	K_2O	TiO_2	P_2O_5	MnO	Cr_2O_3
%	58.7	17.2	10.3	3.82	8.04	3.34	0.82	1.16	0.28	0.16	0.06

Table 4.2: *Composition in basalt rock.*

Although the crystals in this basalt rock are almost randomly oriented, there is a slight preferred orientation, which gives the rock a textural anisotropy this anisotropy measured by doing image analysis of oriented microscope slides cut through the rock by Tony Philpotts. In addition he also measured the degree of anisotropy of a basalt rock by taking the minimum and maximum of magnetic susceptibility where he found at 56.4^0 and 106^0 respectively by considering anisotropy of magnetic susceptibility (AMS), which gives a very accurate measure of the anisotropy of the rock's texture, at least in terms of its response to a low intensity magnetic filed, on the cube of basalt rock. However, the faces of the top

and bottom of the cube crystal which give the most significant results (only 60% probability that shape distribution is isotropic), indicate a maximum elongation in direction of 103^0. This would appear to confirm that, the anisotropy of magnetic susceptibility is caused by the magnetic crystal having anisotropy to their shape or distribution, which in turn must reflect a general textural anisotropy in the specimen. These measurements all confirm that the rock has a textural anisotropy [41]. However, the origin of the anisotropy is not yet explained fully.

Thus, in this work it has been also found that, the minimum and maximum reflected intensities are at 56^0 and 102^0 respectively. After rotating a basalt rock 720^0, by taking North-South direction as reference see fig.6. From this graph one can

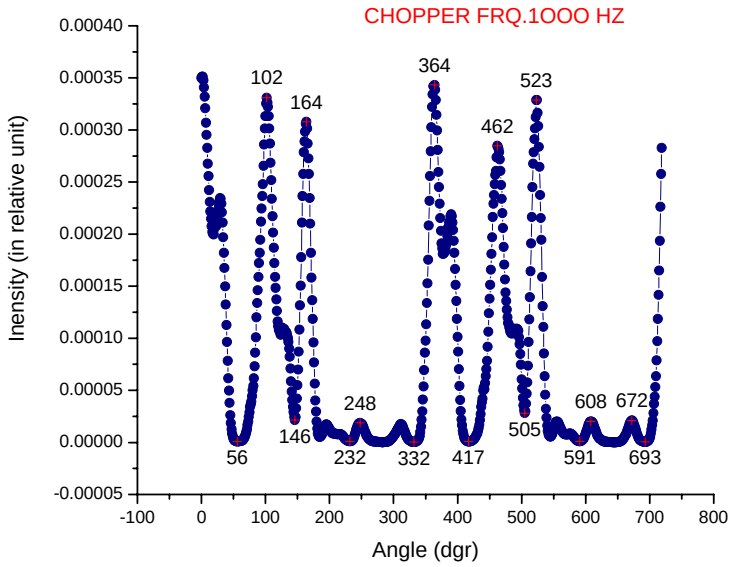

Figure 4.6: *Intensity vs angle for natural basalt rock rotating* 720^0 .

easily realized that, how much the optical technique applied in this research is coincide with the result found by using anisotropy magnetic susceptibility (AMS) at least numerically (see the relation between electric field and magnetic susceptibility from Maxwell's equations). Off course, this very small difference arise, because in the case of AMS experiment, the whole part of rock (bulk) was scanning, but in this work, it has been considered only a single point of the surface of

rock i.e. the center of the rock. Furthermore, it has been attempted to determine the degree of anisotropy by using optical technique RAS. Thus, before expressing the degree of anisotropy of the rock, determination of the optical axis of the crystal is conducted on a well polished basalt rock along 135^0, using the same procedure as for KTP crystal measurements. Then data in fig.4.7 have been found.

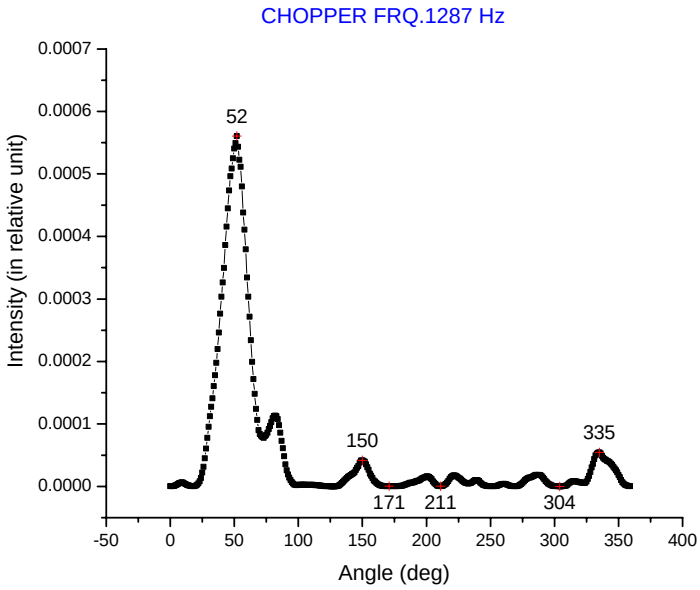

Figure 4.7: *Intensity vs angle for natural basalt rock* .

From fig.4.7 it is easy to observe that the basalt rock is not ideally isotropy crystal, because it is known that for the case of ideally isotropy materials the intensity of reflected light is independent of the angle of rotation of the sample. In addition, as pointed out earlier in this chapter, anisotropy systems should have at least one 2-fold rotation axis (one c_2 symmetry element) but this condition is not observed in the case of this basalt rock because there are a number of different crystals in basalt rock. Therefore, it is possible to realized that the basalt rock has no a long range optical axis at that particular point. Thus, it is difficult to apply RAS technique to get the degree of anisotropy of basalt rock, because the above optical technique is applicable if and only if the sample must have a well

defined and long range optical axis. Further more, in most cases this optical technique is highly applicable for single crystal. But by considering table 4.1 one can simply see that there are so many different compounds in this basalt rock, hence, that may be another case for RAS technique not applicable for this rock. Data recorded from the measurement are given in appendix where $\mid r \mid_1^2$, $\mid r \mid_2^2$ and $\mid r \mid_1^2$ represents Fig.4.1, Fig.4.7 and Fig.4.4 respectively.

Chapter 5

CONCLUSION

When light interact with matter, the reflected light may contains a number of information about that material, especially when the reflected light is analyzed by using sensitive optical techniques like Reflectance Anisotropy Spectroscopy (RAS). In this work the non-distractive optical technique RAS is applied to calculate the degree of anisotropy of KTP crystal. Since KTP crystal have two 2-fold rotation axis (two c_2 symmetry elements) along 0^0 to 181^0 and 154^0 to 338^0, then by considering only one optical axis along 181^0 the degree of anisotropy of KTP crystal is obtained and its value is 3.880×10^{-2} ± 0.00165.

In addition using this optical technique the angle between the two optical axes was determined by rotating the sample 720^0. The angle between the two optical axes for the case of acute angle is calculated and its value is $26^0.0000$ ± 0.0016 and $156^0.0000$ ± 0.0017 for obtuse angle. Furthermore, attempt was made to determine the optical axis of natural basalt rock. However, optical axis could not be determined, because it has no c_2 axis of rotation. But, the angles of minimum and maximum magnetic susceptibility measured by anisotropy magnetic susceptibility is very close to the angle of minimum and maximum intensities of reflected light by using reflectance anisotropy spectroscopy. Since this natural rock is composed of so many compounds and elements, it has more than one crystals with in it, therefore, it has no long range optical axis. But one can determine the degree of anisotropy of this basalt crystal by applying an optical techniques

which are not dependent on the optical axis of the sample like Surface Differential Reflectivity (SDR), 45 Degree Reflectometry (45DR) and others. In this work it is realized that the optical technique RAS is an easy way to characterize an optical axis of crystal.

Finally, the readers of this thesis must be aware of that, this thesis presents basic principles, concepts and applications of RAS for determination of degree of anisotropy of KTP crystal and other related quantities. Here, the descriptions and results are in simplified form, therefore, the readers can find more details information about theoretical and experimental parts in the cited references.

Bibliography

[1] Dieter Schwarzenbach, *Crystallographic*, John Wiley and Sons Ltd. (1996).

[2] Potassium Titanyl Phosphate-KTP: http:// www. st. northropgrumman. com

[3] Potassium Titanyl Phosphate-KTP: http://ece-WWW.colorado.edu

[4] KTP-An oxide of choice for nonlinear optical and electro-optic devices: http:// www. yosh. ac. il

[5] C.V.Kannan, S. Ganesamoorthy and S. Kumaragurubarn, *Cryst. Res. Thchnol.* **37**, (2002), 1049.

[6] J. D. Biorlein and Herman Vanherzeele,*J. Opt. Soc.* **6**, 622, (1989).

[7] D. W. Tenqist, R. M. Whittlee and J. Yarwood, *University Optics*, 2, Gordon and Breach, Science Publishers, INC. (1970).

[8] B. Rossi, *Optics*, Addison-Wesley Publishing Company, INC. (1957).

[9] P. Milloni and J. H. Eberly, *Lasers*, John Wiley, Sons. INC. (1988).

[10] G. R. Fowles, *Introduction to Modern Optics*, 2^{nd} ed., Holt, Rinehart and Winston, INC. (1975).

[11] B. B. Laud, *Electromagnetics*, 2^{nd} ed. (1987).

[12] J. Strong, *Concepts of Classical Optics*, W. H. Freeman and Company INC. (1958).

[13] R. W. Ditchburn, *Light* , 3^{rd} ed., Acadamic Press INC. (1976).

[14] L. Levi, *Applied Optics*,1, John Wiley and Sons. INC. (1968).

[15] E. Hecht, *Optics*, 4^{th} ed., Pearson Education, INC. (2002).

[16] R. M. A. Azzam and N. M. Bashara, *Ellipsometry and Polarized Light*, Elsevier B. V., (1987).

[17] K. W. Kolasinski, *Surface Science:Foundations of Catalysis and Nanoscience*, John Wiley and Sons, LTD. (2002).

[18] D. S. Roseburgh and R. J. Cole,*J. Phys. Condens. Matter* **16**, 4279, (2004).

[19] D. E. Aspnes, J. P. Harbison, A. A. Studna and L .T. Florez,*Appl. Phys. Latt.* **52**, 957, (1988).

[20] L. Bleckmann, O. Hunderi, W. Richter and E. Wold, *Surf. Sci.* **351**, 277, (1996).

[21] W. G. Schmidt, K. Seino, P. H. Hahn, F. Bechsted, W. Lu, S. Wang and J. Bernhole, *Thin Solid Filems*, **455**, 764, (2004).

[22] F. Manghi, R. D. Sole, A. Selloni and E. Molinari, *Phys. Rev. B* **41**, 9935, (1990).

[23] P. Weightman et al, *Rep. Prog. Phys.*, **68**, 1251, (2005).

[24] L. Kipp et, D. k. Biegelsen, J. E. Northrup, L. E. Swartz and R. D. Bringans, *Phys. Rev. Lett.* **76**, 2810, (1996).

[25] W. Dietrich, M. V. der Emde and D. R. T. Zahn, *Semicond. Sci. Technol.* **10**, 1108, (1995).

[26] P. Harrison, T. Farrell, A. Maunder, C. I. Smith and P. Weightman, *Meas. Sci. Technol.*, **12**, 2185, (2001).

[27] *Hinds Instruments of PEM*; http://WWW.hindsinstruments.com.

[28] C. H. Li, Y. Sun, S. B. Visbeck, D. C. Law and R. F. Hicks, *Appl. Phys. Lett.* **81**, 3939, (2002).

[29] T. Yasuda, K. Kimura, S. Miwa and T. Yao, *Phys. Rev. Lett.* **77**, 326, (1996).

[30] Reflectance anisotropy spectroscopy-growth monitoring withsub-monolayer sensitivity: http:// www. laytec. de

[31] D. E. Aspnes and A. A. Studna, *J. Vac. Sci. Technol. A* **5(4)**, 546, (1987).

[32] D. C. Law, Y. Sun and R. F. Hicks, *J. Appl. Phys.* **94**, 6175, (2003).

[33] In-situ characterization of epitaxial semiconductor growt by reflectance anisotrpoy spectroscopy: http:// www. physik, tu-berlin. de.

[34] M. Leibovitch, P.Ram, L. Malikova and F. H. Pollak, *J. Vac. Sci. Technol. B*, **14(4)**, 3089, (1990).

[35] D. E. Aspnes, *Phys. Rev. Lett.* **64**, 192, (1990).

[36] D. E. Aspnes, A. A. Studna, *J. Vac. Sci. Technol. A* **6(3)**, 1327, (1988).

[37] D. E. Aspnes, *J. Vac. Sci. Technol.B* **3(5)**, 1498, (1985).

[38] Crystal Symmetry; http:// www.ig.utexas.edu

[39] Classification of Crystal; http://dx.doi.org

[40] D. Ayalew, Geophyics Dep. of A. A. A, Unpublished report.

[41] Basalt Continuous Fiber:// www.albarrie.com

[42] T. Philpotts, Personal Communication.

DECLARATION

I here by declare that this thesis is my original work and has not been presented for a degree in any other University. All sources of material used for the thesis have been duly acknowledge

_____

Signature of Author

Fekadu Gashaw

June, 2006

This thesis has been submitted for examination with my approval as university advisor.

_____

Signature of advisor

Dr.Araya Asfaw

_____

Signature of advisor

Dr. Mesfin Redi

June, 2006

Appendix

θ	$\|r\|_1^2$	$\|r\|_2^2$	$\|r\|_3^2$	θ	$\|r\|_1^2$	$\|r\|_2^2$	$\|r\|_3^2$	θ	$\|r\|_3^2$	θ	$\|r\|_3^2$
0	0.00135	2.38E-07	0.00492	181	0.00189	6.29E-07	0.00446	361	0.0034	541	0.00542
1	8.62E-04	3.36E-07	0.0047	182	0.00189	6.29E-07	0.00446	362	0.00281	542	0.005
2	4.24E-04	5.82E-07	0.00428	183	0.00189	6.29E-07	0.00446	363	0.00216	543	0.00451
3	4.63E-04	9.55E-07	0.00376	184	0.00189	6.29E-07	0.00446	364	0.00154	544	0.00393
4	9.17E-04	1.64E-06	0.00314	185	0.00189	6.29E-07	0.00446	365	0.00111	545	0.00329
5	0.00163	2.52E-06	0.0025	186	0.00189	6.29E-07	0.00446	366	0.00103	546	0.00263
6	0.00237	3.70E-06	0.0019	187	0.00189	6.29E-07	0.00446	367	0.00134	547	0.00198
7	0.00303	5.10E-06	0.00149	188	0.00189	6.29E-07	0.00446	368	0.00188	548	0.00148
8	0.0036	5.81E-06	0.00137	189	0.00189	6.29E-07	0.00446	369	0.0025	549	0.00127
9	0.00409	6.42E-06	0.00158	190	0.00189	6.29E-07	0.00446	370	0.00311	550	0.00141
10	0.00449	6.11E-06	0.00204	191	0.00189	6.29E-07	0.00446	371	0.00365	551	0.00185
11	0.00481	4.96E-06	0.00261	192	0.00189	6.29E-07	0.00446	372	0.00415	552	0.00242
12	0.00507	3.70E-06	0.00322	193	0.00189	6.29E-07	0.00446	373	0.00455	553	0.00303
13	0.00528	2.52E-06	0.00377	194	0.00189	6.29E-07	0.00446	374	0.00488	554	0.00359
14	0.0054	1.64E-06	0.00424	195	0.00189	6.29E-07	0.00446	375	0.00514	555	0.00407
15	0.00549	1.01E-06	0.00466	196	0.00189	6.29E-07	0.00446	376	0.00536	556	0.00451
16	0.00554	6.29E-07	0.00501	197	0.00189	6.29E-07	0.00446	377	0.00554	557	0.00489
17	0.00558	4.50E-07	0.0053	198	0.00189	6.29E-07	0.00446	378	0.00568	558	0.00517
18	0.00557	4.11E-07	0.00553	199	0.00189	6.29E-07	0.00446	379	0.00579	559	0.00539
19	0.00557	5.82E-07	0.00571	200	0.00189	6.29E-07	0.00446	380	0.00587	560	0.00556
20	0.00549	1.21E-06	0.00583	201	0.00189	6.29E-07	0.00446	381	0.00591	561	0.0057
21	0.0054	2.72E-06	0.00592	202	0.00189	6.29E-07	0.00446	382	0.00593	562	0.00579
22	0.00532	4.96E-06	0.00599	203	0.00189	6.29E-07	0.00446	383	0.00594	563	0.00587
23	0.00523	8.05E-06	0.00602	204	0.00189	6.29E-07	0.00446	384	0.00591	564	0.00592
24	0.00515	1.36E-05	0.00606	205	0.00189	6.29E-07	0.00446	385	0.00589	565	0.00594
25	0.00503	2.21E-05	0.00606	206	0.00189	6.29E-07	0.00446	386	0.00588	566	0.00598
26	0.00492	3.15E-05	0.00605	207	0.00189	6.29E-07	0.00446	387	0.00586	567	0.00597
27	0.00481	4.51E-05	0.00604	208	0.00189	6.29E-07	0.00446	388	0.00585	568	0.00596
28	0.00477	6.06E-05	0.00604	209	0.00189	6.29E-07	0.00446	389	0.00583	569	0.00596
29	0.00476	7.78E-05	0.00602	210	0.00189	6.29E-07	0.00446	390	0.00583	570	0.00593
30	0.00473	9.54E-05	0.006	211	0.00189	6.29E-07	0.00446	391	0.00582	571	0.0059
31	0.00473	1.12E-04	0.006	212	0.00189	6.29E-07	0.00446	392	0.00582	572	0.00588
32	0.00473	1.28E-04	0.00599	213	0.00189	6.29E-07	0.00446	393	0.00583	573	0.00585
33	0.00478	1.41E-04	0.00599	214	0.00189	6.29E-07	0.00446	394	0.00583	574	0.00585
34	0.00482	1.60E-04	0.006	215	0.00189	6.29E-07	0.00446	395	0.00584	575	0.00585
35	0.00489	1.78E-04	0.00602	216	0.00189	6.29E-07	0.00446	396	0.00589	576	0.00584
36	0.00497	1.98E-04	0.00602	217	0.00189	6.29E-07	0.00446	397	0.00594	577	0.00585
37	0.00503	2.20E-04	0.00605	218	0.00189	6.29E-07	0.00446	398	0.006	578	0.00587
38	0.00511	2.46E-04	0.00608	219	0.00189	6.29E-07	0.00446	399	0.00606	579	0.00587
39	0.0052	2.77E-04	0.00614	220	0.00189	6.29E-07	0.00446	400	0.00611	580	0.00588
40	0.00526	3.04E-04	0.00618	221	0.00189	6.29E-07	0.00446	401	0.00615	581	0.00586
41	0.00532	3.26E-04	0.00624	222	0.00189	6.29E-07	0.00446	402	0.00617	582	0.00588
42	0.00541	3.50E-04	0.00629	223	0.00189	6.29E-07	0.00446	403	0.00621	583	0.00589
43	0.0055	3.86E-04	0.00632	224	0.00189	6.29E-07	0.00446	404	0.00626	584	0.00589
44	0.00557	4.16E-04	0.00635	225	0.00189	6.29E-07	0.00446	405	0.00629	585	0.00586
45	0.00566	4.45E-04	0.00636	226	0.00189	6.29E-07	0.00446	406	0.00631	586	0.00586
46	0.00576	4.73E-04	0.0064	227	0.00189	6.29E-07	0.00446	407	0.00633	587	0.00586
47	0.0058	4.96E-04	0.00643	228	0.00189	6.29E-07	0.00446	408	0.00636	588	0.00586
48	0.00586	5.09E-04	0.00646	229	0.00189	6.29E-07	0.00446	409	0.00638	589	0.00584
49	0.00589	5.25E-04	0.00643	230	0.00189	6.29E-07	0.00446	410	0.00636	590	0.00583

50	0.00589	5.41E-04	0.00641	231	0.00189	6.29E-07	0.00446	411	0.00635	591	0.00583
51	0.00588	5.49E-04	0.00641	232	0.00189	6.29E-07	0.00446	412	0.00633	592	0.00584
52	0.00587	5.61E-04	0.00639	233	0.00189	6.29E-07	0.00446	413	0.00631	593	0.00587
53	0.00585	5.44E-04	0.00636	234	0.00189	6.29E-07	0.00446	414	0.00629	594	0.00593
54	0.00583	5.22E-04	0.00637	235	0.00189	6.29E-07	0.00446	415	0.00626	595	0.00599
55	0.00581	5.11E-04	0.00639	236	0.00189	6.29E-07	0.00446	416	0.00627	596	0.00605
56	0.00575	4.80E-04	0.00641	237	0.00189	6.29E-07	0.00446	417	0.00628	597	0.00613
57	0.00569	4.38E-04	0.00645	238	0.00189	6.29E-07	0.00446	418	0.0063	598	0.00621
58	0.00565	4.11E-04	0.0065	239	0.00189	6.29E-07	0.00446	419	0.00634	599	0.00631
59	0.00558	3.79E-04	0.00656	240	0.00189	6.29E-07	0.00446	420	0.0064	600	0.0064
60	0.00555	3.34E-04	0.00662	241	0.00189	6.29E-07	0.00446	421	0.0065	601	0.00648
61	0.00551	3.04E-04	0.00668	242	0.00189	6.29E-07	0.00446	422	0.00658	602	0.00657
62	0.00547	2.72E-04	0.00675	243	0.00189	6.29E-07	0.00446	423	0.00669	603	0.00662
63	0.00547	2.34E-04	0.00683	244	0.00189	6.29E-07	0.00446	424	0.0068	604	0.00666
64	0.00548	2.00E-04	0.0069	245	0.00189	6.29E-07	0.00446	425	0.00691	605	0.00668
65	0.00547	1.71E-04	0.00698	246	0.00189	6.29E-07	0.00446	426	0.00699	606	0.0067
66	0.00548	1.48E-04	0.00706	247	0.00189	6.29E-07	0.00446	427	0.00707	607	0.00669
67	0.00554	1.24E-04	0.00713	248	0.00189	6.29E-07	0.00446	428	0.00714	608	0.00666
68	0.0056	1.06E-04	0.00717	249	0.00189	6.29E-07	0.00446	429	0.00715	609	0.00662
69	0.00567	9.01E-05	0.0072	250	0.00189	6.29E-07	0.00446	430	0.00713	610	0.00657
70	0.00572	8.38E-05	0.00719	251	0.00189	6.29E-07	0.00446	431	0.0071	611	0.00651
71	0.0058	8.11E-05	0.00714	252	0.00189	6.29E-07	0.00446	432	0.00707	612	0.00643
72	0.00588	7.89E-05	0.00713	253	0.00189	6.29E-07	0.00446	433	0.00699	613	0.00633
73	0.00595	7.78E-05	0.00707	254	0.00189	6.29E-07	0.00446	434	0.00689	614	0.00622
74	0.00599	8.05E-05	0.00701	255	0.00189	6.29E-07	0.00446	435	0.00675	615	0.00611
75	0.00599	8.27E-05	0.00691	256	0.00189	6.29E-07	0.00446	436	0.00666	616	0.00603
76	0.00597	8.61E-05	0.00681	257	0.00189	6.29E-07	0.00446	437	0.00655	617	0.00596
77	0.00593	9.18E-05	0.0067	258	0.00189	6.29E-07	0.00446	438	0.00643	618	0.00591
78	0.00584	9.66E-05	0.00659	259	0.00189	6.29E-07	0.00446	439	0.00634	619	0.00589
79	0.00573	1.03E-04	0.00649	260	0.00189	6.29E-07	0.00446	440	0.0063	620	0.00588
80	0.00559	1.09E-04	0.00643	261	0.00189	6.29E-07	0.00446	441	0.00626	621	0.00589
81	0.00546	1.13E-04	0.00637	262	0.00189	6.29E-07	0.00446	442	0.00622	622	0.00591
82	0.00532	1.13E-04	0.00633	263	0.00189	6.29E-07	0.00446	443	0.00619	623	0.00592
83	0.00519	1.12E-04	0.00632	264	0.00189	6.29E-07	0.00446	444	0.0062	624	0.00592
84	0.00506	1.08E-04	0.0063	265	0.00189	6.29E-07	0.00446	445	0.00622	625	0.00592
85	0.00498	9.78E-05	0.0063	266	0.00189	6.29E-07	0.00446	446	0.00623	626	0.00592
86	0.00489	8.61E-05	0.00629	267	0.00189	6.29E-07	0.00446	447	0.00622	627	0.00588
87	0.00483	7.30E-05	0.00627	268	0.00189	6.29E-07	0.00446	448	0.00619	628	0.00582
88	0.00481	6.10E-05	0.00626	269	0.00189	6.29E-07	0.00446	449	0.00614	629	0.00574
89	0.0048	4.84E-05	0.00619	270	0.00189	6.29E-07	0.00446	450	0.00607	630	0.00568
90	0.00478	3.50E-05	0.00608	271	0.00189	6.29E-07	0.00446	451	0.00596	631	0.0056
91	0.00476	2.60E-05	0.00598	272	0.00189	6.29E-07	0.00446	452	0.00585	632	0.00553
92	0.00471	1.93E-05	0.00583	273	0.00189	6.29E-07	0.00446	453	0.00573	633	0.00548
93	0.00465	1.41E-05	0.00566	274	0.00189	6.29E-07	0.00446	454	0.0056	634	0.00545
94	0.00456	1.01E-05	0.0055	275	0.00189	6.29E-07	0.00446	455	0.0055	635	0.00541
95	0.00443	6.89E-06	0.00536	276	0.00189	6.29E-07	0.00446	456	0.00543	636	0.00543
96	0.00426	4.44E-06	0.00523	277	0.00189	6.29E-07	0.00446	457	0.00539	637	0.00549
97	0.00405	2.92E-06	0.00516	278	0.00189	6.29E-07	0.00446	458	0.0054	638	0.00557
98	0.00383	2.24E-06	0.00514	279	0.00189	6.29E-07	0.00446	459	0.00544	639	0.00564
99	0.0036	2.15E-06	0.00515	280	0.00189	6.29E-07	0.00446	460	0.00554	640	0.0057
100	0.00336	2.33E-06	0.00521	281	0.00189	6.29E-07	0.00446	461	0.00564	641	0.00575

101	0.00313	2.52E-06	0.00531	282	0.00189	6.29E-07	0.00446	462	0.00575	642	0.0058
102	0.00295	2.72E-06	0.00543	283	0.00189	6.29E-07	0.00446	463	0.00586	643	0.0058
103	0.00283	2.82E-06	0.00557	284	0.00189	6.29E-07	0.00446	464	0.00598	644	0.00577
104	0.0028	2.72E-06	0.00571	285	0.00189	6.29E-07	0.00446	465	0.00607	645	0.00571
105	0.00285	2.72E-06	0.00584	286	0.00189	6.29E-07	0.00446	466	0.00617	646	0.0056
106	0.00297	2.52E-06	0.00595	287	0.00189	6.29E-07	0.00446	467	0.00622	647	0.00545
107	0.00314	2.42E-06	0.00605	288	0.00189	6.29E-07	0.00446	468	0.00627	648	0.00528
108	0.00336	2.42E-06	0.00611	289	0.00189	6.29E-07	0.00446	469	0.0063	649	0.0051
109	0.00357	2.52E-06	0.00617	290	0.00189	6.29E-07	0.00446	470	0.0063	650	0.00487
110	0.00379	2.42E-06	0.00622	291	0.00189	6.29E-07	0.00446	471	0.00626	651	0.00463
111	0.004	2.24E-06	0.00623	292	0.00189	6.29E-07	0.00446	472	0.00622	652	0.00437
112	0.0042	2.24E-06	0.00622	293	0.00189	6.29E-07	0.00446	473	0.00615	653	0.00411
113	0.00438	2.15E-06	0.00621	294	0.00189	6.29E-07	0.00446	474	0.00608	654	0.00383
114	0.00454	2.15E-06	0.00618	295	0.00189	6.29E-07	0.00446	475	0.00599	655	0.00355
115	0.00469	1.89E-06	0.00615	296	0.00189	6.29E-07	0.00446	476	0.00586	656	0.00325
116	0.00482	1.64E-06	0.0061	297	0.00189	6.29E-07	0.00446	477	0.00575	657	0.00295
117	0.00494	1.35E-06	0.00605	298	0.00189	6.29E-07	0.00446	478	0.00562	658	0.00267
118	0.00503	1.01E-06	0.00599	299	0.00189	6.29E-07	0.00446	479	0.0055	659	0.00238
119	0.00513	7.83E-07	0.00593	300	0.00189	6.29E-07	0.00446	480	0.00538	660	0.00211
120	0.00523	5.36E-07	0.00588	301	0.00189	6.29E-07	0.00446	481	0.00526	661	0.0019
121	0.00533	4.11E-07	0.00583	302	0.00189	6.29E-07	0.00446	482	0.00513	662	0.00174
122	0.00541	3.01E-07	0.00579	303	0.00189	6.29E-07	0.00446	483	0.00503	663	0.0016
123	0.00549	2.10E-07	0.00574	304	0.00189	6.29E-07	0.00446	484	0.00494	664	0.00146
124	0.00559	1.82E-07	0.00572	305	0.00189	6.29E-07	0.00446	485	0.00487	665	0.00134
125	0.00566	1.34E-07	0.00571	306	0.00189	6.29E-07	0.00446	486	0.00482	666	0.00122
126	0.00573	9.30E-08	0.00571	307	0.00189	6.29E-07	0.00446	487	0.0048	667	0.00115
127	0.00581	7.56E-08	0.00573	308	0.00189	6.29E-07	0.00446	488	0.0048	668	0.00106
128	0.00588	7.56E-08	0.00576	309	0.00189	6.29E-07	0.00446	489	0.00482	669	9.58E-04
129	0.00594	1.58E-07	0.00579	310	0.00189	6.29E-07	0.00446	490	0.00487	670	8.62E-04
130	0.006	3.01E-07	0.00584	311	0.00189	6.29E-07	0.00446	491	0.00492	671	7.59E-04
131	0.00605	6.79E-07	0.00591	312	0.00189	6.29E-07	0.00446	492	0.00498	672	6.57E-04
132	0.00608	1.72E-06	0.00597	313	0.00189	6.29E-07	0.00446	493	0.00506	673	5.45E-04
133	0.0061	3.13E-06	0.00603	314	0.00189	6.29E-07	0.00446	494	0.00516	674	4.60E-04
134	0.00613	5.10E-06	0.00609	315	0.00189	6.29E-07	0.00446	495	0.00528	675	3.84E-04
135	0.00614	7.38E-06	0.00615	316	0.00189	6.29E-07	0.00446	496	0.0054	676	3.12E-04
136	0.00613	9.50E-06	0.00622	317	0.00189	6.29E-07	0.00446	497	0.0055	677	2.92E-04
137	0.00613	1.15E-05	0.00629	318	0.00189	6.29E-07	0.00446	498	0.00561	678	3.33E-04
138	0.00612	1.36E-05	0.00635	319	0.00189	6.29E-07	0.00446	499	0.00575	679	4.07E-04
139	0.00608	1.55E-05	0.00642	320	0.00189	6.29E-07	0.00446	500	0.0059	680	5.41E-04
140	0.00602	1.67E-05	0.00646	321	0.00189	6.29E-07	0.00446	501	0.00601	681	7.39E-04
141	0.00593	1.80E-05	0.00648	322	0.00189	6.29E-07	0.00446	502	0.00611	682	9.94E-04
142	0.00582	1.96E-05	0.00651	323	0.00189	6.29E-07	0.00446	503	0.0062	683	0.0013
143	0.00565	2.10E-05	0.0065	324	0.00189	6.29E-07	0.00446	504	0.00628	684	0.00165
144	0.00548	2.24E-05	0.00646	325	0.00189	6.29E-07	0.00446	505	0.00635	685	0.00202
145	0.00525	2.63E-05	0.00642	326	0.00189	6.29E-07	0.00446	506	0.00639	686	0.00239
146	0.00496	2.98E-05	0.00633	327	0.00189	6.29E-07	0.00446	507	0.00642	687	0.00276
147	0.00462	3.29E-05	0.00622	328	0.00189	6.29E-07	0.00446	508	0.00642	688	0.00316
148	0.00422	3.80E-05	0.00606	329	0.00189	6.29E-07	0.00446	509	0.0064	689	0.00356
149	0.00374	4.15E-05	0.00587	330	0.00189	6.29E-07	0.00446	510	0.00634	690	0.00393
150	0.00321	4.19E-05	0.00563	331	0.00189	6.29E-07	0.00446	511	0.00627	691	0.00427
151	0.00265	4.11E-05	0.00533	332	0.00189	6.29E-07	0.00446	512	0.00614	692	0.00457

152	0.00202	3.95E-05	0.00499	333	0.00189	6.29E-07	0.00446	513	0.00599	693	0.00483
153	0.00148	3.50E-05	0.00461	334	0.00189	6.29E-07	0.00446	514	0.00579	694	0.00506
154	0.00122	3.05E-05	0.00417	335	0.00189	6.29E-07	0.00446	515	0.00556	695	0.00527
155	0.00132	2.66E-05	0.00366	336	0.00189	6.29E-07	0.00446	516	0.00526	696	0.00543
156	0.00179	2.04E-05	0.00309	337	0.00189	6.29E-07	0.00446	517	0.00491	697	0.00554
157	0.00244	1.70E-05	0.00253	338	0.00189	6.29E-07	0.00446	518	0.0045	698	0.00561
158	0.00321	1.34E-05	0.00206	339	0.00189	6.29E-07	0.00446	519	0.00402	699	0.00563
159	0.00395	9.50E-06	0.00181	340	0.00189	6.29E-07	0.00446	520	0.00349	700	0.0056
160	0.0046	7.71E-06	0.00185	341	0.00189	6.29E-07	0.00446	521	0.00292	701	0.00552
161	0.00517	5.81E-06	0.0022	342	0.00189	6.29E-07	0.00446	522	0.00234	702	0.00537
162	0.00567	4.06E-06	0.00276	343	0.00189	6.29E-07	0.00446	523	0.0019	703	0.00518
163	0.00606	2.72E-06	0.0034	344	0.00189	6.29E-07	0.00446	524	0.00172	704	0.00482
164	0.00636	1.80E-06	0.00404	345	0.00189	6.29E-07	0.00446	525	0.00185	705	0.00441
165	0.00658	1.01E-06	0.0046	346	0.00189	6.29E-07	0.00446	526	0.00229	706	0.00392
166	0.00672	6.79E-07	0.00507	347	0.00189	6.29E-07	0.00446	527	0.00291	707	0.00332
167	0.0068	4.50E-07	0.00548	348	0.00189	6.29E-07	0.00446	528	0.00357	708	0.00259
168	0.0068	3.36E-07	0.00581	349	0.00189	6.29E-07	0.00446	529	0.00417	709	0.00175
169	0.00672	2.38E-07	0.00606	350	0.00189	6.29E-07	0.00446	530	0.00471	710	8.82E-04
170	0.00658	2.38E-07	0.00623	351	0.00189	6.29E-07	0.00446	531	0.00518	711	4.04E-04
171	0.00636	2.38E-07	0.00633	352	0.00189	6.29E-07	0.00446	532	0.00557	712	5.31E-04
172	0.00609	2.69E-07	0.00636	353	0.00189	6.29E-07	0.00446	533	0.00588	713	0.00112
173	0.00574	3.01E-07	0.00632	354	0.00189	6.29E-07	0.00446	534	0.0061	714	0.00192
174	0.00532	3.01E-07	0.00621	355	0.00189	6.29E-07	0.00446	535	0.00623	715	0.0027
175	0.00481	3.01E-07	0.00602	356	0.00189	6.29E-07	0.00446	536	0.0063	716	0.0034
176	0.00423	3.01E-07	0.00575	357	0.00189	6.29E-07	0.00446	537	0.00627	717	0.00397
177	0.00354	3.72E-07	0.0054	358	0.00189	6.29E-07	0.00446	538	0.00616	718	0.00443
178	0.00275	4.93E-07	0.00496	359	0.00189	6.29E-07	0.00446	539	0.006	719	0.0048
179	0.00189	6.29E-07	0.00446	360			0.00394	540	0.00575		
180	0.00189	6.29E-07	0.00446								